

RESEARCH

Open Access



Transcriptome-wide high-throughput deep m⁶A-seq reveals unique differential m⁶A methylation patterns between three organs in *Arabidopsis thaliana*

Yizhen Wan^{1,2*}, Kai Tang^{2†}, Dayong Zhang^{4†}, Shaojun Xie^{2,3}, Xiaohong Zhu^{2,3}, Zegang Wang⁵ and Zhaobo Lang^{2,3*}

Abstract

Background: m⁶A is a ubiquitous RNA modification in eukaryotes. Transcriptome-wide m⁶A patterns in *Arabidopsis* have been assayed recently. However, differential m⁶A patterns between organs have not been well characterized.

Results: Over two-third of the transcripts in *Arabidopsis* are modified by m⁶A. In contrast to a recent observation of m⁶A enrichment in 5' mRNA, we find that m⁶A is distributed predominantly near stop codons. Interestingly, 85 % of the modified transcripts show high m⁶A methylation extent compared to their transcript level. The 290 highly methylated transcripts are mainly associated with transporters, stress responses, redox, regulation factors, and some non-coding RNAs. On average, the proportion of transcripts showing differential methylation between two plant organs is higher than that showing differential transcript levels. The transcripts with extensively higher m⁶A methylation in an organ are associated with the unique biological processes of this organ, suggesting that m⁶A may be another important contributor to organ differentiation in *Arabidopsis*. Highly expressed genes are relatively less methylated and *vice versa*, and different RNAs have distinct m⁶A patterns, which hint at mRNA fate. Intriguingly, most of the transposable element transcripts maintained a fragmented form with a relatively low transcript level and high m⁶A methylation in the cells.

Conclusions: This is the first study to comprehensively analyze m⁶A patterns in a variety of RNAs, the relationship between transcript level and m⁶A methylation extent, and differential m⁶A patterns across organs in *Arabidopsis*.

Keywords: N⁶-methyladenosine, m⁶A mapping, Transcriptome-wide patterns, RNA differential methylation, Transposable element

Background

Over 100 types of chemical modifications have been discovered in RNAs from all of the living species [1, 2]. The most diverse modifications were present in ribosomal RNA (rRNA) and transfer RNA (tRNA). Chemical modifications are also prevalent in messenger RNA (mRNA) and other non-coding RNA (ncRNA) in eukaryotes [1, 2]. Among those, the most important is

modified by N⁶-methyladenosine (m⁶A) [2–4]. m⁶A has been found ubiquitously distributed in rRNA, tRNA, mRNA, and some snRNA of eukaryotes, such as yeast [5], mammals [4, 6], insects [2], and plants [7]. Recently, transcriptome-wide analyses showed that one-third of the transcribed genes (mRNA) were modified by m⁶A in human and mouse [4, 6, 8]. The m⁶A enriched sites were found near stop codons, in 3'UTRs and mRNA segments derived from large exons [4, 6, 8]. These studies also showed that this modification was highly conserved in eukaryotes [2, 6], suggesting that a delicate regulatory mechanism may be responsible for this selective modification, and provided clues of the important metabolisms that this modification involved in or was responsible for,

* Correspondence: wuz689@hotmail.com; lang.zhaobo@foxmail.com

†Equal contributors

¹State Key Lab Laboratory of Crop Stress Biology for Arid Areas, College of Horticulture, College of Life Sciences, Northwest A&F University, Yangling, Shaanxi 712100, China

²Department of Horticulture and Landscape Architecture, Purdue University, West Lafayette, IN 47907, USA

Full list of author information is available at the end of the article

for example, RNA splicing [6, 8], RNA export [4], and RNA stability [4, 6].

The availability of antibody that specifically binds the m⁶A modified sites and efficiently enriches RNAs containing m⁶A modification facilitates the transcriptome-wide analysis of the patterns of this RNA modification through the biotechnologies of RNA sequencing (RNA-seq), RNA immunoprecipitation (RIP), and m⁶A-seq [4, 6, 8]. RIP was primarily used to analyze RNA-protein interaction [9]. However, the aim of the RIP experiment for the m⁶A-seq study was to pull down the RNA of interest containing m⁶A modification through application of m⁶A antibody to the randomly fragmented RNA pool. m⁶A-seq is a recently reported technology integrating the powers of both RIP and high-throughput RNA sequencing for transcriptome-wide analysis of m⁶A methylation patterns in eukaryotes [6, 10].

Transcriptome-wide analysis of m⁶A in mammals and plants provided insights into topological patterns and facilitated discovery of some functions of this RNA modification [4, 6, 10–13]. However, the differential m⁶A methylation among plant organs, for example, leaves, flowers, and roots, has not been well characterized. In this study, we significantly improved biotechnologies for RNA isolation and RIP, thus deep and high quality m⁶A-seq and massively m⁶A-mapped datasets in *Arabidopsis* are now available. This study aimed to: (1) comprehensively and transcriptome-wide characterize the m⁶A distributing patterns in numerous types of RNAs in *Arabidopsis*; (2) analyze the relationship between the transcript level and the m⁶A modification extent in the *Arabidopsis* transcriptome; (3) characterize differential patterns of the m⁶A methylation among leaves, flowers, and roots; and (4) discuss new functions of m⁶A modification in the transcripts extensively modified by m⁶A from the clues of the potential biological functions in these transcripts. This is the first study to comprehensively analyze m⁶A differential patterns across organs in plants. This study opens up a new avenue to greatly understand the transcriptome-wide patterns of m⁶A modification in different RNAs, relationship between m⁶A methylation extent and gene transcript level, and m⁶A differential patterns across organs in plants.

Results

Quality and depth of the RNA sequencing in this study

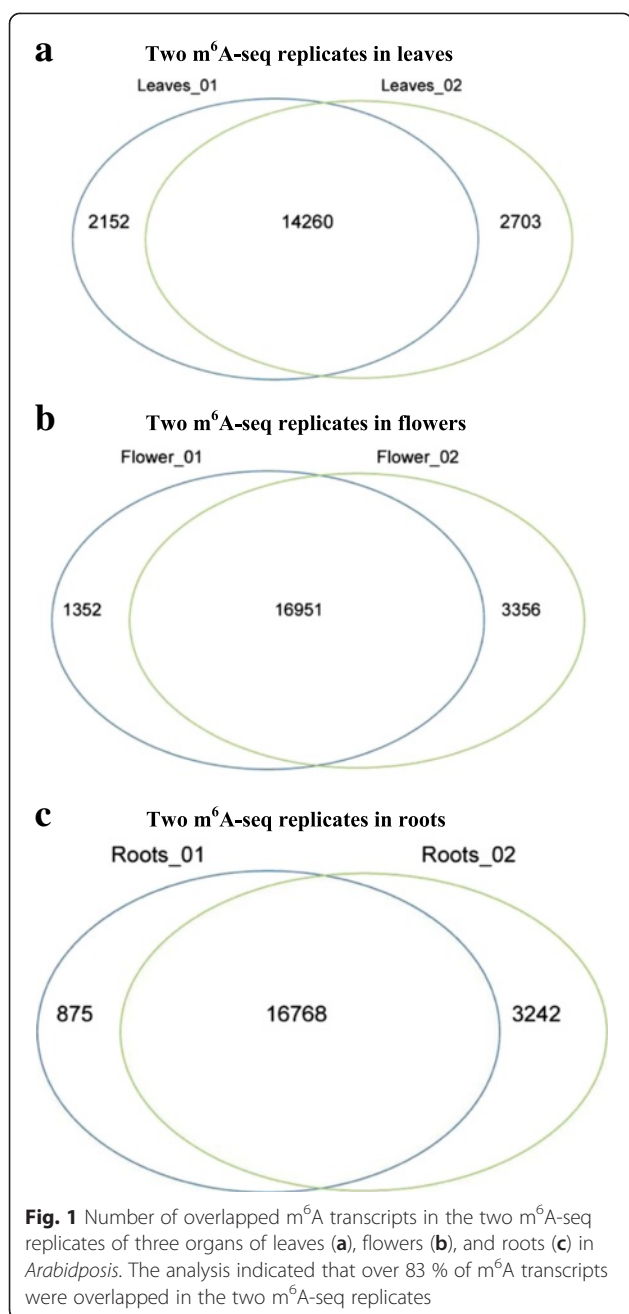
Commercial m⁶A antibody has proved to specifically bind to m⁶A RNA and has been successfully used for the m⁶A RNA immunoprecipitation experiments in the previous studies [4, 6, 10–13]. In this study, we collected samples from three organs of *Arabidopsis*: leaves, flowers, and roots; and performed m⁶A-seq, mRNA-seq, and input RNA-seq (total fragmented RNA without RIP experiments for sequencing and as the control for m⁶A-seq) with two

replicates for each sample (Additional file 1). A total of 90 to 156 million reads were generated for each m⁶A-seq sample; 48 to 92 million reads for each mRNA-seq sample and 25 to 53 million reads for each input RNA-seq sample (Additional file 1). The proportion of the cleanly mapped reads and transcripts in m⁶A-seq were around 65–70 % (Additional file 1). Compared to m⁶A-seq data in the mammalian (11 to 24 million reads for each sample) [6] and in the rice (23 to 47 million reads for each sample) [12], the depth of the m⁶A-seq in this study (Additional file 1) was greatly high. The HPLC-MS/MS results indicated that RIP efficiency for m⁶A enrichment was high in this study (Additional file 2), and the non-specific immunoprecipitation rate was extensively low (lower than 1 %) in this study (Additional file 2), suggesting that the experimental error caused by non-precipitation was also low in the m⁶A-seq in this study.

General features and extent of m⁶A methylation in *Arabidopsis*

We identified that 16,688 to 19,305 transcripts were modified by m⁶A in the three *Arabidopsis* organs. For all three organs, at least 83 % agreement was found between two m⁶A-seq replicates in this study (Fig. 1). This agreement proportion between replicates was the highest compared to the previous reports [6, 13]. We found that 70.6 %, 73.7 %, and 76.7 % of the transcribed genes (transcripts) were chemically modified by m⁶A in the leaves, flowers and roots of *Arabidopsis*, respectively (Additional file 3). This estimation was greatly higher than previous reports (over one-third) in human, mouse [6] and (approximately 50 %) plant [13]. The estimation differences may be due to the different criteria used for calling of the ‘m⁶A modified transcripts’ in m⁶A-seq [6, 13]. In the previous studies, input data were used as the control for calling the m⁶A modified transcripts due to relatively high non-specific immuno-precipitation rate in their experiments. This could result in underestimation of both total m⁶A peaks and proportion of the m⁶A transcripts in the transcriptome [6, 13]. However, all the mapped reads after removal of PCR duplicates in the m⁶A-seq were counted and considered to be derived from RNA fragments containing m⁶A modification in this study. And thus the transcripts with m⁶A mapped reads were considered as the modified transcripts due to very low non-specific immuno-precipitation rate (lower than 1 %) in this study (Additional file 2). But our estimation may better reflect the m⁶A modification extent in the cells (see details in the Discussion section of this paper).

On average of two replicates, over 80 % of the m⁶A modified transcripts were common among the leaves, flowers, and roots (Fig. 2). On average, around 32,300



m⁶A sites from the leaves, approximately 43,400 sites from the flowers, and approximately 48,100 from the roots were successfully mapped to the *Arabidopsis* genome with an estimation of approximately 2.0 to 2.6 m⁶A sites per m⁶A transcript and approximately 1.4 to 2.0 m⁶A sites per transcript in the whole transcriptome (Additional file 4). This estimation was comparable to that in mammals (approximately 1.5 m⁶A sites per transcript) [6], but higher than the estimated in the plant (0.7 to 1.0 m⁶A site per transcript) [13]. However our observation was closer to the earlier reports, for example, approximately 3-5 m⁶A sites per transcript [1, 2]. The ratio

of m⁶A/A in the m⁶A modified transcripts was in the range of 0.44 % to 0.61 % in the three organs, and this ratio was in a range of 0.35 % to 0.50 % in the whole transcriptome of three organs in *Arabidopsis* (Additional file 5). This ratio estimation is also comparable to the recently reported in the plant [13].

m⁶A topological patterns in *Arabidopsis*

Over two-third of the methylated transcripts exhibited one or two m⁶A sites (Fig. 3a, details in Additional file 6). And over 17 % contained four or more sites (Fig. 3a, details in Additional file 6), which was much higher than previously reported (only 5.5 %) in human [6].

The consensus sequence of m⁶A modification has been identified as 'RRm⁶ACH', where R is A/G and H is A/C/U [4, 6, 14]. Our data showed that over 75 % of the RIP fragments in the m⁶A-seq contained the consensus sequence RRm⁶ACH in *Arabidopsis* (Fig. 3b). The most two frequent motifs were AAm⁶ACU (19.3 %) and AAm⁶ACA (19.0 %) (Fig. 3b). This observation is consistent with the recent reports in plants [12, 13].

The m⁶A topology in mRNA was categorized into two types according to the m⁶A patterns distributing in the whole transcript. One type was characterized by dominant m⁶A enrichment observed at stop codon or 3'UTR. And 73.0 % to 76.3 % of the mRNA in three organs was modified by this type of the m⁶A pattern (Fig. 4a, Additional file 7). Thus, most of the methylated mRNA was characterized by this typical m⁶A topology in *Arabidopsis* (Type 1, Fig. 4a): one or two high peaks at stop codon or at 3'UTR with extremely low m⁶A signals observed in the coding regions. In most cases, the peak height in 3'UTR or at stop codon was two to a dozen of folds of the signal heights in the coding regions (Fig. 4a, Fig. 5). This dominant m⁶A enrichment was not found in the remaining mRNA (Type 2, Fig. 4b). The overall m⁶A signals were also relatively low in Type 2 (Fig. 4b). Transcriptome-wide analysis showed that the overall m⁶A patterns distributing within genes were highly close with each other among three organs (Fig. 5). Statistic analysis indicated that the normalized read depth representing the overall m⁶A patterns had non-significant differences among three organs ($P = 0.716$, Additional file 8), suggesting that recognition of motif for m⁶A methylation was extensively conserved among plant organs.

Two types of m⁶A patterns were observed in rRNAs: one was modified by one m⁶A site, and the other was methylated by several m⁶A sites (Fig. 6a and b). The m⁶A topology in tRNAs was also categorized into two major types: approximately 10 % of tRNAs were slightly modified by m⁶A (Fig. 6c) and m⁶A methylation was not observed in the remaining tRNAs. Both snRNA and snoRNA were highly methylated by m⁶A, but only a single m⁶A site was found in these two types of RNAs

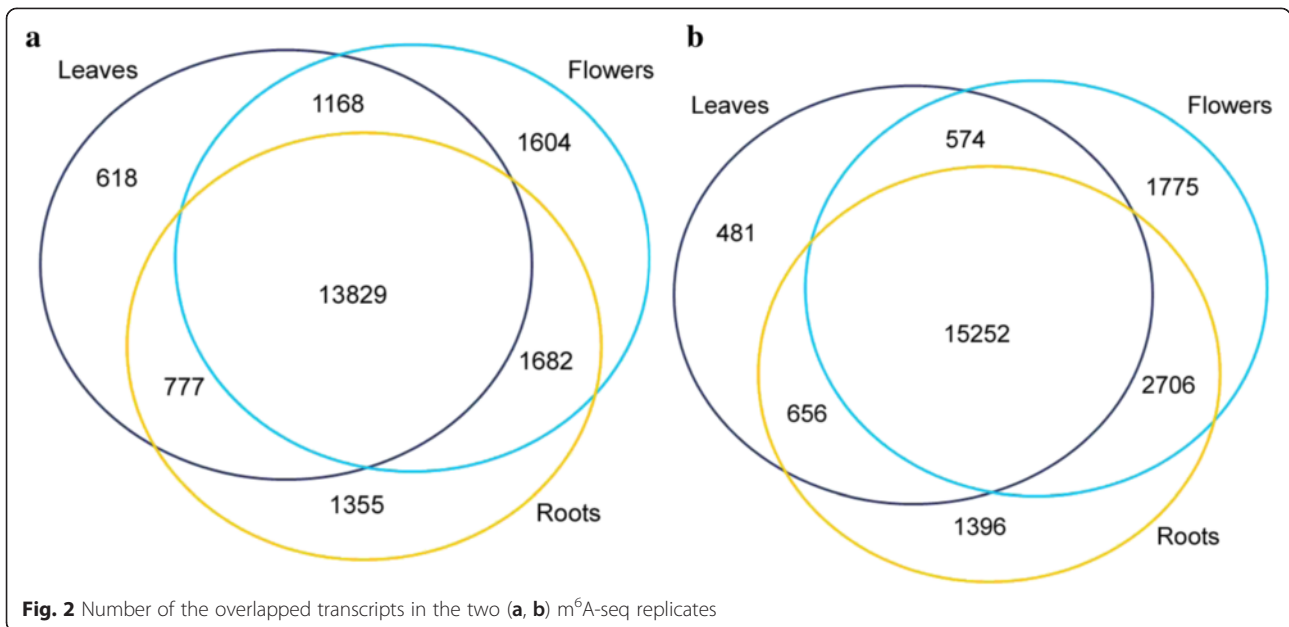
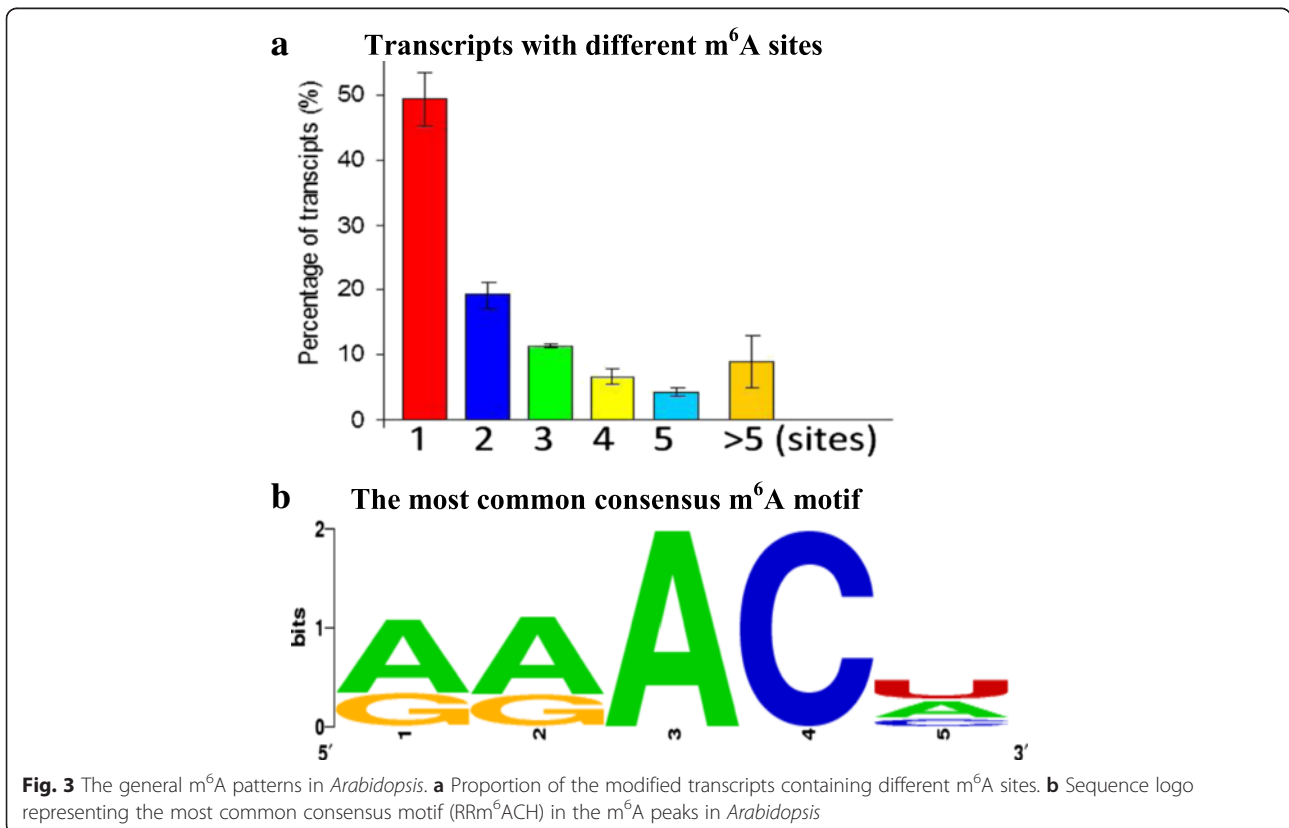


(Fig. 6d). Therefore, different types of RNAs were endowed with distinct m⁶A topologies.

m⁶A methylation extent versus gene transcript level

To compare m⁶A methylation extent in m⁶A-seq with gene transcript level (TL) in mRNA-seq in three organs

of *Arabidopsis*, we categorized the m⁶A methylation extent into three groupings based on the comparison of modified Fragments Per Kilobase of Transcript Per Million Fragments Mapped (MFPKM) of the transcript in the m⁶A-seq with the FPKM of the counterpart in the mRNA-seq using χ^2 test (to test whether ratio of



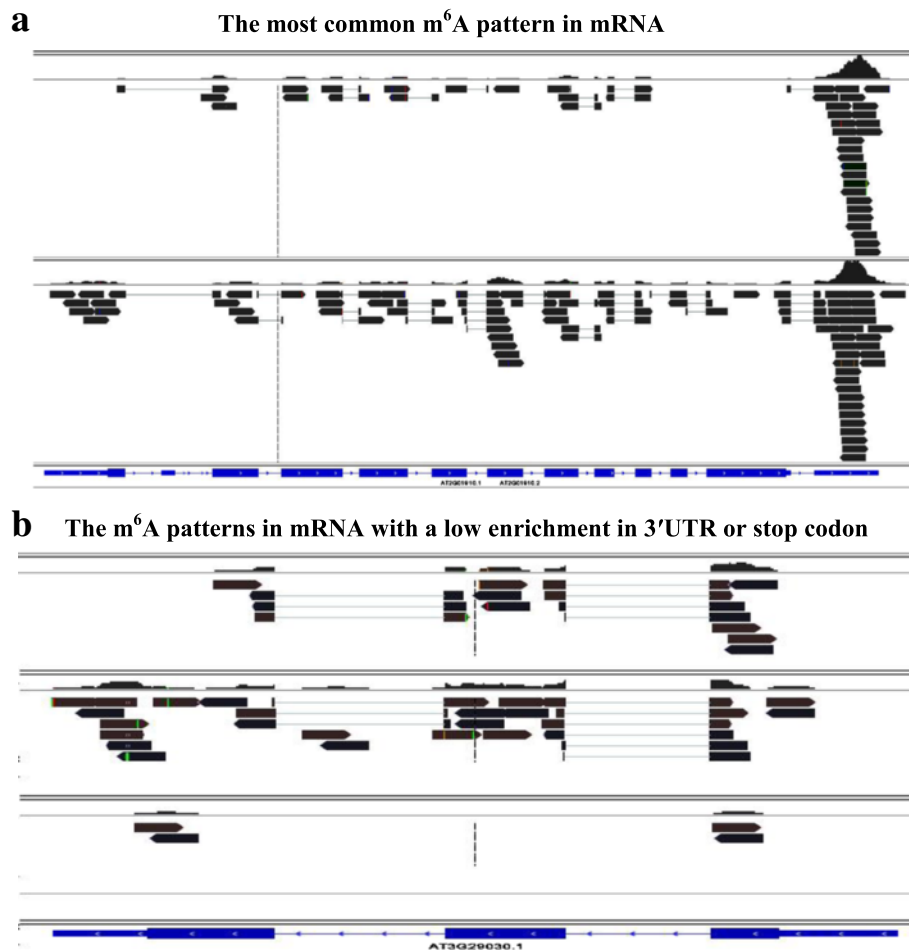


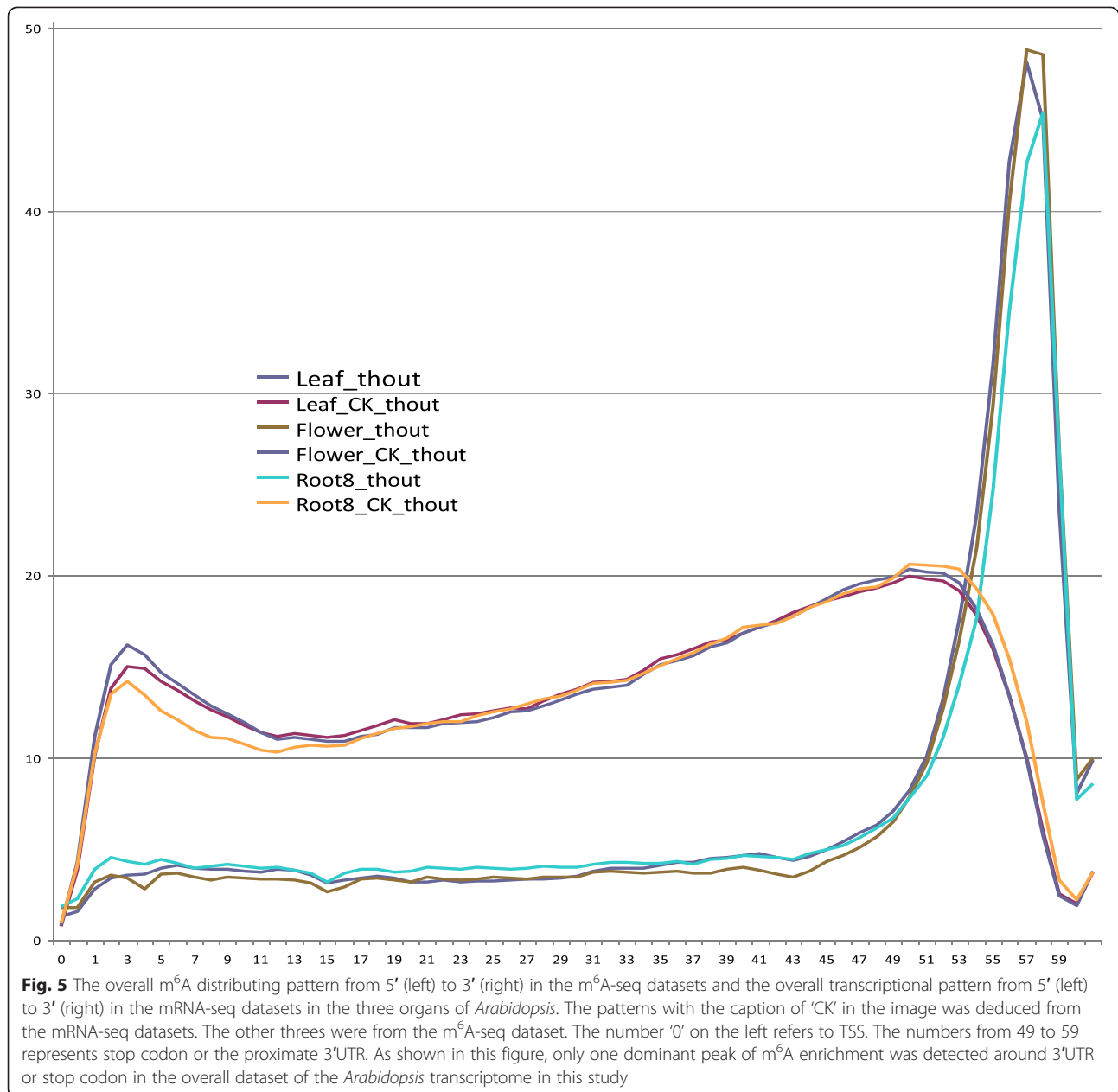
Fig. 4 Schematic screen shots of two typical types of m⁶A topologies in mRNA in *Arabidopsis*. **a** Type 1 (representative gene, 'AT2G01910'; trace files of two organs (flowers and roots) were presented), one or two predominant peaks in 3'UTR or at stop codon with several much lower signals in the codon regions. The peaks in 3'UTR or at stop codon were two to tens of folds of the signals in the codon regions. Most of the messenger RNA (over 70 %) presented this type of m⁶A topology. **b** Type 2 (representative gene, 'At3g29030'; trace files of three organs, leaves (the upper), flowers (in the middle), and roots (the lower) were presented). Several m⁶A sites distributing in the transcripts with low m⁶A signals (in the middle and lower parts of the figure, representative of flowers and roots) or without peaks in 3'UTR or at stop codon (in the upper part, representative of leaves)

MFPKM to FPKM in each transcript fits 1:1 in each organ, $P < 0.05$ (Table 1). The ratio of MFPKM to FPKM is higher (or lower) than 1 by χ^2 test ($P < 0.05$), representing that the m⁶A methylation extent in m⁶A-seq was relatively high (or low) compared to the transcript level in mRNA-seq. When the ratio of MFPKM to FPKM in each transcript fits 1:1 ($P < 0.05$), the m⁶A methylation extent was considered relatively 'equivalent' to the transcript level. This comparison was applied to estimate the m⁶A methylation extent of a transcript compared to its transcript level. All the m⁶A methylated transcripts were used for this estimation and the transcripts without m⁶A methylation detected were excluded for this comparison.

Interestingly, 83.4 % to 89.1 % of the methylated transcripts showed a high m⁶A modification level, while <4 % of the m⁶A modified transcripts had a low modification

extent versus their transcript level in mRNA-seq in the three organs (Table 1). Thus, most of the m⁶A modified transcripts showed a relatively high m⁶A modification extent versus their gene transcript level in the three organs of *Arabidopsis*.

To further analyze relationship between the m⁶A methylation extent in m⁶A-seq and the transcript level in mRNA-seq in three organs of *Arabidopsis*, the transcript level was categorized into three groupings: high, moderate and low. Each category contained one-third of the m⁶A modified transcripts from the highest to the lowest FPKM in mRNA-seq. The comparison of ratio of the average MFPKM in m⁶A-seq to the average FPKM in mRNA-seq between three groupings using *t*-test (Table 2) showed that most of the highly expressed transcripts were relatively less modified by m⁶A, and most



transcripts with a low expression level were more likely modified by m⁶A ($P < 0.005$). The moderately expressed transcripts tended to be moderately methylated in *Arabidopsis* ($P < 0.005$). This observation somewhat differed from the report in human and mouse: the moderately expressed transcripts were more likely to be methylated, and those expressed at the two extremes were less methylated by m⁶A [6]. Both of our two groups used the similar methods to analyze the relationship between the m⁶A methylation extent and the gene expression level [6]. The reasons causing the differences may not be due to different methodologies or different biological species because a number of studies have proved that m⁶A methylation is

highly conserved among eukaryotes [2, 6, 8, 12]. However, our observation may authentically reflect m⁶A methylation in the cells: the genes with a lower transcript level may require a relatively higher m⁶A modification extent to maintain RNA stability in the cells [12, 13] and *vice versa*.

We found that approximately 5.5 % of the m⁶A modified transcripts were extensively methylated by m⁶A in each organ (with fold change (ratio of MFPKM in the m⁶A-seq to FPKM in the mRNA-seq) ≥ 10 , false discovery rate (FDR) $< 10^{-12}$, and read number per transcript ≥ 30). And 290 (2.1 %) extensively m⁶A methylated transcripts were found common in all of the three organs of

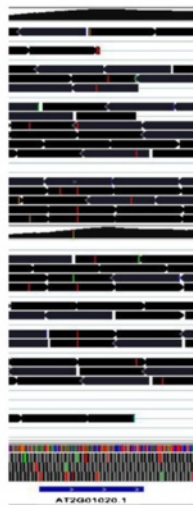
a Numerous m⁶A sites in rRNA**b** One m⁶A site in rRNA**c** Low m⁶A in tRNA**d** One m⁶A site in sn(o)RNA

Fig. 6 Schematic screen shots of the m⁶A patterns in rRNA, tRNA and sn(o)RNA. **a** Numerous m⁶A sites distributed in a rRNA transcript (representative 'AT2g01010'). **b** A single m⁶A in a rRNA transcript (representative 'AT2g01020'). **c** Low m⁶A methylation in most of tRNA (approximately 90 %, representative 'AT1g06480'). **d** sn(o) RNA was highly methylated by a single m⁶A site (representative 'AT3G56705')

leaves, flowers, and roots in *Arabidopsis*. These transcripts extensively modified by m⁶A were mainly associated with transporter, defenses or stress response, redox, nucleic acid binding, signal transduction, regulation of transcription, DNA/RNA/protein modification, cell proliferation or cycle, transposable element gene, pseudogenes, and snRNA (Table 3) [15–63]. Gene ontology (GO) analysis showed that the major molecular functions in these

transcripts were responsible for molecule binding, transferase, hydrolase, stress responses, transporter, and kinase activity (Fig. 7).

Differential m⁶A methylation among leaves, flowers, and roots

High m⁶A sequencing depth (reads) of a transcript in the m⁶A-seq dataset may not suggest that this transcript

Table 1 Three groupings of the m⁶A methylation extent compared to the transcript level in three organs of the *Arabidopsis* m⁶A transcriptome

Replicates	Plant organs	High		Low		Equivalent	
		Transcripts (n)	Proportion (%)	Transcripts (n)	Proportion (%)	Transcripts (n)	Proportion (%)
Replicate 1	Leaves	13,711	83.5	606	3.7	2,094	12.8
	Flowers	14,807	80.8	762	4.2	2,760	15.0
	Roots	14,275	80.9	413	2.3	2,955	16.7
	Average		81.7		3.4		14.8
Replicate 2	Leaves	16,067	94.7	98	0.6	798	4.7
	Flowers	18,764	92.4	100	0.5	1,443	7.1
	Roots	17,188	85.9	485	2.4	2,337	11.7
	Average		91.0		1.2		7.8

'High', 'Low', and 'Equivalent' were categorized by comparison of the m⁶A-seq depth (MFPKM, the methylation extent of m⁶A) of each transcript with that in the mRNA-seq (FPKM, the transcript level). 'High' or 'Low' referred to as a relatively high or low m⁶A methylation extent compared with its transcript level based on χ^2 test ($P < 0.05$); 'Equivalent', suggested that the m⁶A methylation depth was relatively 'equivalent' to the transcript level (ratio of MFPKM to FPKM fits 1:1) based on χ^2 test ($P < 0.05$)

was highly methylated by m⁶A in the cells because the gene transcript level of the counterpart may also be relatively high in the mRNA-seq dataset. To minimize effect of gene transcript level on estimation of m⁶A methylation extent of the transcripts and to more precisely evaluate differential m⁶A methylation among organs, we applied an algorithm 'NFPKM' to each transcript to estimate differential m⁶A methylation among three organs (see details in the Methods section of this paper). Two fold change and chi-square were applied for estimation of differential m⁶A methylation between organs using our algorithm. Accordingly, these two criteria were also used to estimate differential gene transcripts in mRNA-seq and to have a parallel comparison with the results of differential m⁶A methylation among organs in this study.

On average, 26.6 % of the transcripts presented differential in mRNA-seq (fold change of FPKM between two organs >2 or <0.5 , and FDR <0.05), while 33.5 % showed differential methylation between two organs (fold change of NFPKM between two organs >2 or <0.5 , and FDR <0.05)

(Table 4). A paired analysis indicated that ratio of transcripts showing differential m⁶A methylation was significantly higher than that showing the differential gene transcripts in the three *Arabidopsis* organs ($P < 0.00035$). The comparison also showed that the leaves had the highest extent of m⁶A methylation among three organs followed by the flowers. And the roots were less likely methylated among three organs (Table 4).

Eleven genes were randomly chosen for validation of our analysis above (Additional file 9). As products of qRT-PCR cover a short span in the transcriptome (50 to 150 bp) [13], two flanks of the amplicon containing one m⁶A peak in IGV program and showing differential m⁶A methylation were chosen to design primers (Additional file 9). The correlation coefficient between the qRT-PCR relative abundance results and the RIP-seq expected abundances was significant ($r = 0.8632$ (r between 0.7738-0.9526 for 95 % CI), $n = 33$ genes, and $P < 10^{-4}$), indicating that our qRT-PCR data were consistent with the data estimated by m⁶A-seq and mRNA-seq using the IGV program (Additional file 10).

Table 2 Relationship between the m⁶A methylation extent and the transcript level in three organs of the *Arabidopsis* m⁶A transcriptome

Replicates	Plant organs	High			Moderate			Low		
		MFPKM	FPKM	Ratio	MFPKM	FPKM	Ratio	MFPKM	FPKM	Ratio
Replicate 1	Leaves	232.23	75.65	3.07	146.87	29.17	5.03	76.96	7.66	10.05
	Flowers	206.13	65.15	3.16	137.14	28.56	4.80	68.52	8.68	7.89
	Roots	156.63	62.28	2.51	111.23	28.44	3.91	56.22	7.35	7.65
Replicate 2	Leaves	221.14	88.55	2.50	176.68	17.94	9.84	99.06	3.75	26.42
	Flowers	152.77	80.11	1.91	120.33	15.29	7.87	69.34	3.49	19.87
	Roots	98.93	83.58	1.18	65.81	11.74	5.61	45.53	2.22	20.49

'High', 'Moderate', and 'Low' refer to three groupings of the transcript levels from the highest to the lowest FPKM in mRNA-seq. Each grouping included one-third numbers of the m⁶A modified transcripts. t -test on ratio of the average MFPKM in m⁶A-seq to the average FPKM in mRNA-seq in each grouping showed significantly different ($P < 0.005$) ratios between three groupings

Table 3 Potential functions in the 290 transcripts presenting extensively high methylation in all of the three organs of leaves, flowers and roots in *Arabidopsis*

Potential functions ^a	Gene ID	References ^b
Transporter	AT1G23900, AT1G06470, AT1G60070, AT1G79610, AT2G07671, AT2G07687, AT2G07698, AT2G07741, AT2G41700, AT3G08650, AT3G08960, AT3G17430, AT3G20560, AT3G20920, AT3G46830, AT4G00630, AT4G00800, AT4G38920, AT4G39850, AT5G27970, AT5G36940, AT5G53530, AT5G01990, AT3G55320, AT4G13750, AT1G16820, AT1G77140, AT5G05570, AT5G07770, AT2G21340, AT2G27460, AT1G74720, AT1G47550, AT5G66380, AT5G47490, AT5G08470, AT3G03720, AT5G61310, AT5G62600, AT5G11980, AT1G56290, AT2G20840, AT2G15240, AT4G39420, AT5G07980,	[15–21]
Defense or stress response	AT1G63770, AT1G64790, AT1G67090, AT1G80030, AT2G05580, AT2G27380, AT2G35510, AT2G42560, AT3G20290, AT3G22640, AT3G49600, AT4G01210, AT4G04920, AT4G08230, AT4G25520, AT4G33650, AT5G10450, AT5G11530, AT5G14030, AT5G14790, AT5G34850, AT5G35620, AT5G43460, AT5G63110, AT3G46920, AT1G10522, AT2G46240, AT1G58220, AT1G57870, AT1G01260, AT1G67890, AT4G31390, AT3G54610, AT1G74720, AT1G80010, AT1G31835, AT1G50730, AT4G05631	[18, 22–33]
Redox process	AT1G50430, AT1G67140, AT1G76150, AT2G27110, AT1G80560, AT2G07687, AT2G07727, AT2G38020, AT3G20560, AT2G48060, AT4G08280, AT4G23420, AT4G39850, AT5G42790, AT5G65750, AT4G01860, AT3G08950, AT3G01380, AT4G36080, AT2G43420, AT4G16310, AT5G21060, AT1G56000, AT4G17150, AT5G08470, AT4G16070, AT4G30993, AT3G20560	[18, 34–36]
Signal transduction	AT1G03060, AT1G43130, AT1G48090, AT1G51690, AT1G58250, AT3G46830, AT3G49600, AT4G38200, AT5G06260, AT5G28900, AT5G35180, AT5G49470, AT5G39760, AT2G15240, AT3G55850, AT1G13180, AT1G10522, AT1G67890, AT5G07770, AT5G06350, AT4G02970, AT1G58230, AT2G46700, AT3G18040, AT5G07770, AT1G74720	[19, 28, 33, 37–39]
Nucleic acid binding, DNA repair, DNA/RNA synthesis	AT1G02990, AT1G08840, AT1G12930, AT1G50840, AT2G20000, AT2G32000, AT1G17580, AT3G54280, AT1G20920, AT1G58060, AT2G19520, AT3G23780, AT3G48190, AT3G61240, AT4G09680, AT4G25880, AT5G05560, AT5G16630, AT5G22010, AT2G03070, AT3G23780, AT3G53500, AT1G07705, AT4G00060, AT4G16280, AT4G32200, AT1G33390, AT3G54460	[18, 40–43]
Regulation of transcription	AT1G07470, AT2G20330, AT2G35110, AT3G53500, AT4G04920, AT5G42770, AT5G49470, AT5G63260, AT1G07705, AT1G53541, AT5G39760, AT1G17450, AT1G10522, AT5G13240, AT1G58220, AT1G01260, AT5G08230, AT2G48110, AT1G33390, AT5G08550, AT2G36960, AT3G61740, AT3G10070, AT5G49430	[18, 30, 44]
DNA methylation, demethylation, and gene silencing	AT1G08060, AT1G54490, AT2G06210, AT3G01460, AT4G16280, AT3G07610, AT5G05570	[18, 45, 46]
Cell proliferation, circadian rhythm, or differentiation	AT1G17110, AT1G17580, AT1G22620, AT1G22770, AT1G67490, AT2G25730, AT2G26890, AT2G35110, AT3G07160, AT3G49600, AT5G06265, AT5G11030, AT5G12980, AT5G24740, AT5G40740, AT5G42770, AT5G51290, AT2G19390, AT1G55540, AT3G15120, AT5G10340, AT5G48120, AT1G77460, AT4G13750, AT3G27670, AT4G32200, AT4G04970, AT3G19630, AT4G18600, AT1G11060, AT4G02070, AT1G67140	[18, 21, 40, 47–51]
Protein phosphorylation or histone acetylation	AT1G13320, AT1G16710, AT1G49340, AT5G04510, AT5G18525, AT5G49470, AT3G46920, AT1G31860, AT1G57870, AT4G31390, AT2G46700, AT3G18040	[18, 52, 53]
Protein post translational process, for example, folding, ubiquitination	AT1G62330, AT3G06440, AT3G18520, AT3G56120, AT3G59410, AT4G33650, AT5G05920, AT5G06260, AT5G11530, AT5G51660, AT5G63110, AT1G79940, AT1G80030, AT1G73950, AT3G60350, AT5G07910, AT3G54610, AT1G80010, AT3G46220, AT3G20560, AT1G56290	[18, 54, 55]

Table 3 Potential functions in the 290 transcripts presenting extensively high methylation in all of the three organs of leaves, flowers and roots in *Arabidopsis* (Continued)

RNA post-transcriptional processing	AT1G24050, AT1G24706, AT1G31870, AT1G32500, AT1G64572, AT3G11540, AT1G35470, AT1G73720, AT3G11960, AT3G19670, AT3G47890, AT3G53500, AT3G53500, AT5G51660, AT3G56825, AT3G57570, AT3G19515, AT3G19630, AT3G13290, AT5G10370, AT4G02970, AT5G62600, AT3G55220, AT3G10070	[18, 56–59]
Proteolysis or protein synthesis	AT1G67120, AT1G67550, AT2G40930, AT4G26510, AT5G35620, AT5G58200, AT5G23110, AT1G28350, AT5G49030, AT5G27700, AT3G47060, AT2G07715, AT2G24640, AT2G25740	[18]
Protein located in mitochondria or chloroplast	AT1G09980, AT1G58350, AT1G68160, AT2G01008, AT2G07671, AT2G07708, AT2G07687, AT2G07727, AT2G11910, AT2G31141, AT2G33980, AT2G35750, AT2G07698, AT3G12590, AT3G41762, AT3G50380, AT4G00585, AT4G02770, AT4G31350, AT4G38120, AT4G39690, AT5G08060, AT5G15320, AT5G15750, AT5G26850, AT5G59613, AT1G07705, AT3G58010, AT3G63052, AT1G30910, AT3G08950, AT3G47060, AT2G07715, AT1G10522, AT3G06310, AT1G31860, AT5G53740, AT1G49700, AT4G31390, AT2G21340, AT3G43540, AT2G25660, AT5G66380, AT1G45332, AT5G61310, AT5G15700, AT3G18040, AT3G56120, AT4G01210, AT4G00630, AT4G13730, AT4G38920, AT5G53530, AT1G63770	[17, 18, 28, 29, 60–63]
Transposable element gene	AT3G28945, AT4G06477, AT4G08114, AT4G08115, AT5G35935, AT3G42806, AT4G16870, AT4G08112	
Pseudogenes	AT2G07709, AT2G07711, AT2G07717, AT2G07733, AT2G07811, AT2G07747, AT2G35743	
sn (o) RNA or other ncRNA	AT1G15405, AT1G08115, AT3G56705, AT5G09585, AT5G61455, AT3G55485, AT2G01020, AT1G16635, AT2G01010, AT2G43375, AT3G56825, AT2G46192, AT5G06165, AT1G61275, AT4G39363, AT3G41979, AT1G12013	
RNA post-transcriptional processing	AT1G24050, AT1G24706, AT1G31870, AT1G32500, AT1G64572, AT3G11540, AT1G35470, AT1G73720, AT3G11960, AT3G19670, AT3G47890, AT3G53500, AT3G53500, AT5G51660, AT3G56825, AT3G57570, AT3G19515, AT3G19630, AT3G13290, AT5G10370, AT4G02970, AT5G62600, AT3G55220, AT3G10070	[18, 56–59]

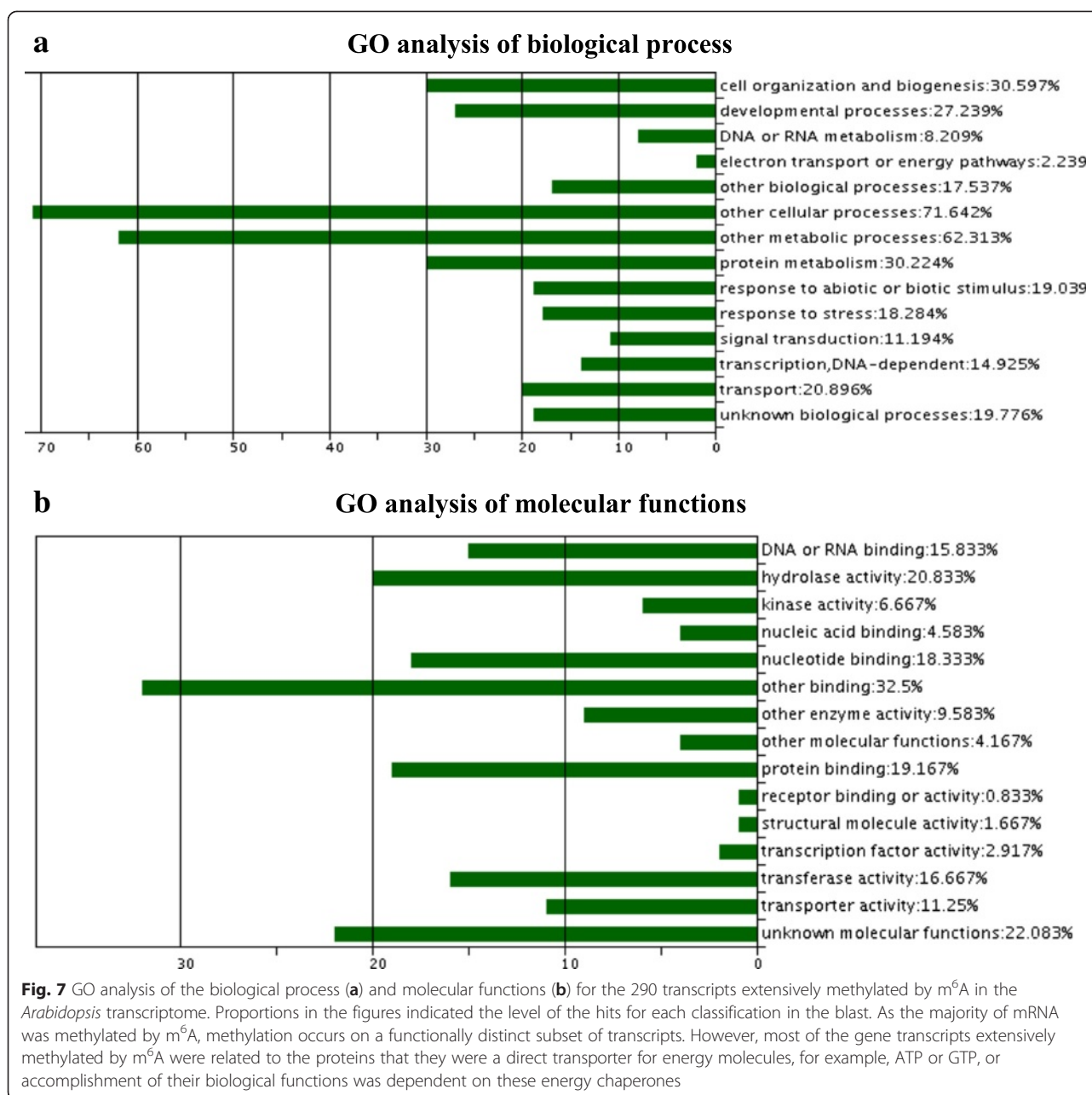
^aSuggests the function of RNA itself, for example, rRNA, or the functions in its expressed proteins

^bThe functions of many transcripts were inferred by gene ontology (GO) analysis using the online tool in TAIR (<http://www.arabidopsis.org/>) and some functions were inferred from the recent publications

The heatmap representing the overall patterns of both differential transcript level and m⁶A methylation extent revealed completely distinct patterns: (1) between transcript level and m⁶A methylation; (2) among three organs; (3) among different genes; (4) among different regions on the same or different chromosomes; and (5) among five chromosomes (Fig. 8). This suggested that both differential gene transcripts and differential m⁶A methylation were highly heterogeneous in the *Arabidopsis* transcriptome and that regulation of the gene transcript level and extent of RNA m⁶A methylation may be relatively independent events.

Analysis of common elements between two replicate datasets showed that 2,628 (18.1 %) m⁶A modified transcripts in leaves, 1,920 (13.5 %) in flowers, and 1,166 (8.0 %) in roots showed a higher extent of methylation than the other two organs (fold change of NFPKM between two organs >2 or <0.5, FDR <0.05). Based on GO analysis, the major molecular functions in these transcripts were relevant to binding activity, transferase,

hydrolase, kinase, transporter, and transcription factor (Fig. 9). Based on KEGG pathway analysis, certain transcripts presenting higher methylation in leaves than the other two organs were related to pathways of photosynthesis, carbohydrate, and nitrogen metabolism (Table 5); transcripts with higher methylation in flowers were concerning metabolic pathways of RNA degradation, DNA replication, and protein synthesis metabolisms (Table 5); transcripts presenting higher methylation in roots involved in biosynthesis of alkaloids, and carbonate metabolism (Table 5) (fold change of NFPKM between two organs >2 or <0.5, FDR <0.005). We found that 43 transcripts in leaves, 41 in flowers, and 23 in roots showed an extensively higher methylation level than the other two organs (fold change of NFPKM between two organs ≥10 or <0.1, FDR <10⁻¹⁰, and read number per transcript ≥20). The transcripts extensively methylated in leaves were mainly expressed for proteins located in mitochondria or chloroplast, photosynthesis, regulation of transcription, or stress response (Table 6)



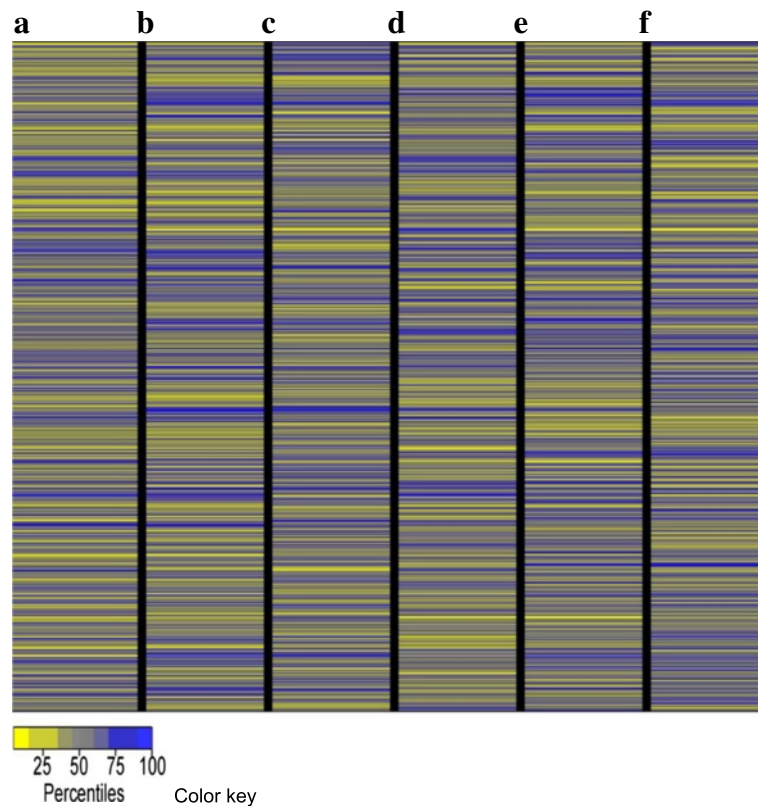
[64–71]; those in flowers (Table 7) were differentially or specifically expressed in the reproductive organs during flowering, or for cell proliferation, circadian rhythm, protein metabolism, transporter, or defense response [72–88]; and those in roots were mainly expressed for defense or stress response, transporters, redox process, or signaling transduction (Table 8) [89–100]. Therefore, the transcripts representing extensively higher m⁶A methylation in an organ revealed an intriguing phenomenon that functions of these transcripts were required for or highly related with unique biological roles of this organ (Tables 6, 7, and 8).

Gene transcript level and m⁶A RNA methylation patterns in the transposable element genes

Interestingly, more than 97 % of the transcripts from the transposable element gene (TE) exhibited relatively high extent of m⁶A modification compared to gene transcript level (fold change of NFPKM between two organs >2 or <0.5, FDR <0.05). Another intriguing phenomenon was that most (>75 %) of the TE transcripts presented a ‘fragmented’ form in the both m⁶A-seq and mRNA-seq data (Fig. 10). The transcript level was distinct among the fragmented TE transcripts, though the transcript fragments were derived from the same TE in the genome

Table 4 The gene transcripts presenting differential transcript level and differential m⁶A methylation across three organs in *Arabidopsis* (fold change >2 or <0.5, FDR <0.05)

Replicates and differential transcripts			Leaves vs. Flowers		Leaves vs. Roots		Flowers vs. Roots	
			Hi-leaves	Hi-flowers	Hi-leaves	Hi-leaves	Hi-flowers	Hi-root
Differential transcript level	Replicate 1	Transcripts (n)	893	1,826	1,706	1,869	2,070	1,148
		Proportion (%)	6.5	13.2	12.3	13.5	15.0	8.3
		Total (%)	19.7		25.8		23.3	
	Replicate 2	Transcripts (n)	1,728	2,671	2,724	2,031	3,068	1,626
		Proportion (%)	11.3	17.5	17.9	13.3	20.1	10.7
		Total (%)	28.8		31.2		30.8	
Differential m ⁶ A methylation	Replicate 1	Transcripts (n)	2,273	1,601	2,857	1,537	2,451	1,649
		Proportion (%)	16.4	11.6	20.7	11.1	17.7	11.9
		Total (%)	28.1		31.2		29.6	
	Replicate 2	Transcripts (n)	4,004	1,268	4,819	1,869	4,576	1,062
		Proportion (%)	26.3	8.3	31.6	12.3	30.0	7.0
		Total (%)	34.6		43.8		37.0	

**Fig. 8** Heatmap by the gene alphabetic order presenting the overall differential patterns of both gene transcript and m⁶A methylation level in the transcripts in *Arabidopsis*. **a** Overview of the differential patterns of m⁶A methylation between leaves and flowers. **b** Overview of the differential patterns of m⁶A methylation between leaves and roots. **c** Overview of the differential patterns of m⁶A methylation between flowers and roots. **d** Overview of the differential patterns of gene transcript level between leaves and flowers. **e** Overview of the differential patterns of gene transcript level between leaves and roots. **f** Overview of the differential patterns of gene transcript level between flowers and roots. The patterns in all of the six comparisons (**a** to **f**) above were based on the alphabetic order of the gene ID representing Chromosomes 1 to 5 (up to down)

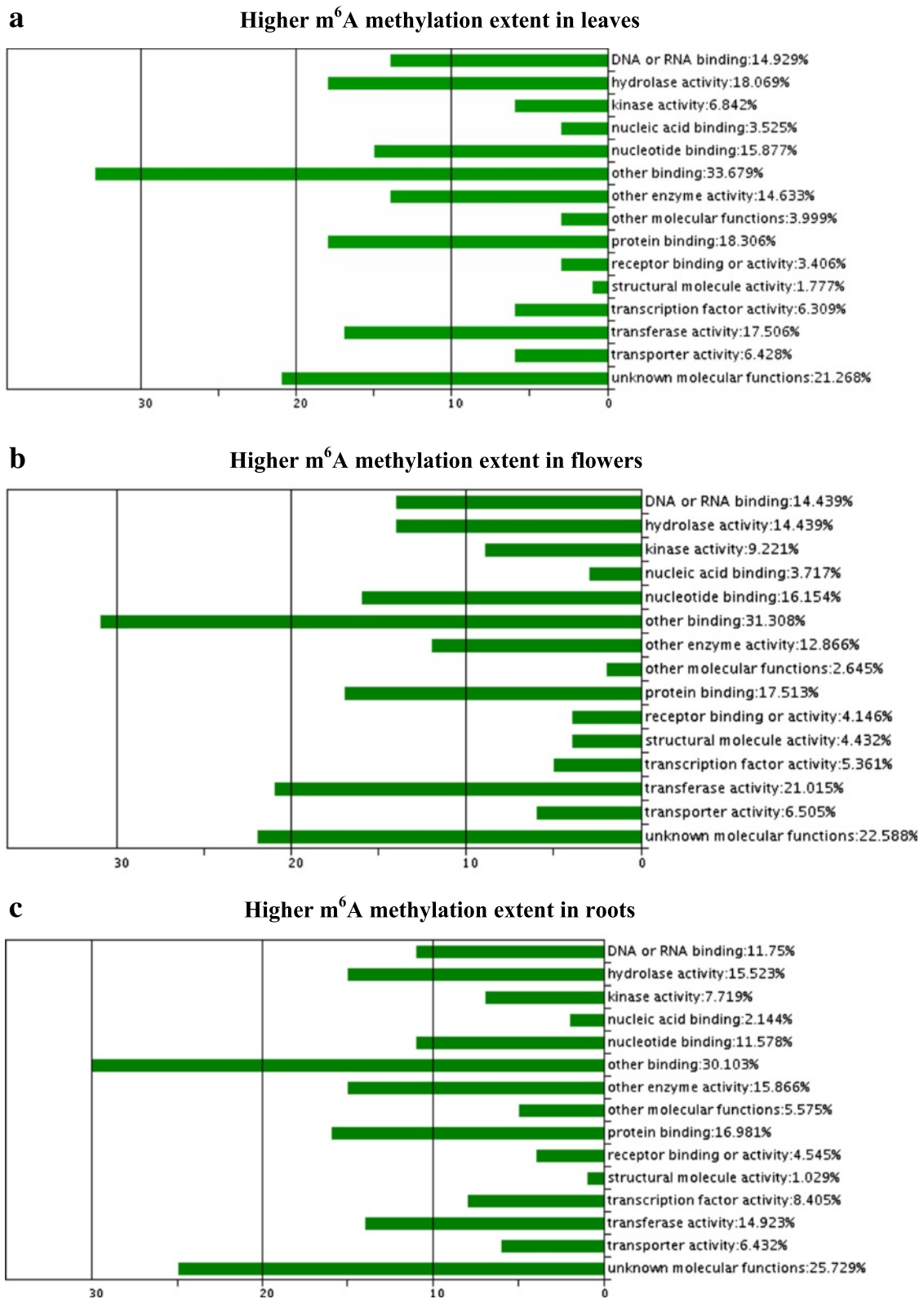


Fig. 9 GO analysis of molecular functions of transcripts presenting a higher extent of m⁶A methylation in leaves (a), flowers (b), or roots (c) than other two organs in *Arabidopsis*

Table 5 KEGG pathways of the transcripts representing a higher methylation extent in one organ than the other two organs in *Arabidopsis*

Organs	Pathways	Count	Hit (%)	P value	Genes
Higher in leaves	Photosynthesis	16	0.66	3.72E-11	AT3G47470, AT1G29920, AT1G29930, AT1G61520, AT3G54890, AT3G27690, AT1G15820, AT3G08940, AT5G54270, AT4G10340, AT2G05100, AT2G34430, AT2G34420, AT2G05070, AT3G61470, AT5G01530
	Photosynthesis	28	1.15	3.01E-08	AT1G30380, AT2G20260, AT1G44575, AT5G66570, AT4G03280, AT4G05180, AT4G04640, AT1G76100, AT1G31330, AT1G03130, AT4G32260, AT1G52230, AT4G12800, AT4G02770, AT1G06680, AT1G60950, AT1G79040, AT1G55670, AT1G20340, AT4G09650, AT5G66190, AT1G15700, AT5G64040, AT3G16140, AT1G67740, AT4G28750, AT1G32550, AT3G50820
	Carbon fixation in photosynthetic organisms	23	0.94	4.67E-05	AT1G70580, AT3G55800, AT2G21170, AT5G65690, AT3G12780, AT3G54050, AT2G01290, AT2G45290, AT2G19900, AT5G61410, AT3G60750, AT5G11520, AT5G38410, AT5G38420, AT3G26650, AT1G32060, AT1G67090, AT1G68750, AT3G47520, AT5G38430, AT4G38970, AT5G52920, AT3G04790
	Nitrogen metabolism	11	0.45	0.03	AT3G03910, AT3G01500, AT3G23490, AT5G35630, AT2G28210, AT1G77760, AT5G14740, AT1G70410, AT1G11860, AT3G47340, AT2G41560
	Glycosaminoglycan degradation	4	0.16	0.03	AT5G13690, AT1G05590, AT5G27730, AT1G65590
	Glyoxylate and dicarboxylate metabolism	9	0.37	0.03	AT3G21720, AT3G47520, AT5G38430, AT5G03860, AT5G38410, AT4G17360, AT3G14415, AT5G38420
Higher in flowers	RNA degradation	7	0.60	0.03	AT5G38890, AT1G03330, AT3G07750, AT1G65700, AT1G03360, AT1G80780, AT3G03710
	DNA replication and protein synthesis	19	1.63	0.05	AT2G34480, AT5G64650, AT1G56045, AT3G25520, AT1G80750, AT3G09500, AT3G04840, AT4G34620, AT3G28500, AT5G02610, AT4G31985, AT2G01250, AT2G19720, AT2G04390, AT1G61580, AT2G25210, AT1G07070, AT5G39850, AT1G78630
Higher in roots	Flavonoid biosynthesis	9	0.46	1.33E-05	AT5G07990, AT1G74550, AT4G34050, AT5G42800, AT2G30490, AT3G55120, AT5G08640, AT5G13930, AT4G22880
	Carbonate metabolism	13	0.66	0.003	AT3G55800, AT3G54050, AT4G37870, AT4G26520, AT2G19900, AT4G26530, AT5G38420, AT1G42970, AT5G09660, AT5G11670, AT5G38430, AT1G12900, AT4G38970
	Biosynthesis of phenylpropanoids	28	1.43	0.006	AT1G74550, AT1G18870, AT3G54050, AT5G28237, AT4G26530, AT1G42970, AT2G37040, AT5G50950, AT4G34230, AT1G51680, AT5G47000, AT3G17070, AT2G37130, AT4G26520, AT5G51890, AT1G15950, AT5G07990, AT5G09660, AT3G21240, AT4G34050, AT1G12900, AT4G38970, AT2G30490, AT3G53260, AT3G55120, AT5G08640, AT5G13930, AT4G22880
	alpha-Linolenic acid metabolism	7	0.36	0.009	AT4G15440, AT3G45140, AT2G35690, AT2G06050, AT1G55020, AT1G76680, AT3G25780
	Phenylpropanoid biosynthesis	14	0.72	0.02	AT1G74550, AT3G17070, AT2G37130, AT5G51890, AT1G15950, AT4G34050, AT3G21240, AT2G37040, AT2G30490, AT3G53260, AT4G34230, AT2G22990, AT1G51680, AT5G47000
	Tropane, piperidine and pyridine alkaloid biosynthesis	5	0.26	0.03	AT2G29320, AT2G37040, AT2G29360, AT2G29340, AT3G53260
	Stilbenoid, diarylheptanoid and gingerol biosynthesis	10	0.51	0.03	AT1G74550, AT4G37310, AT4G34050, AT3G26220, AT3G26200, AT2G30490, AT5G04660, AT3G53280, AT3G26280, AT3G26290

Table 6 Potential functions of the 43 transcripts presenting extensively higher m⁶A methylation in leaves than that in the other two organs in *Arabidopsis* (fold change >10 or <0.1, FDR <10⁻¹⁰)

Potential functions ^a	Gene ID	References ^b
Carbohydrate metabolism	AT1G33700, AT5G13000	[18]
Photosynthesis metabolism or photomorphogenesis	AT1G55670, AT2G05100, AT3G08940, AT3G21055, AT1G67740, AT1G03130, AT2G34420, AT1G15820, AT4G10340, AT1G61520, AT2G06520, AT3G27690, AT3G15190, AT1G14790	[64–66]
Defense or stress response	AT4G35770, AT5G66570, AT2G05520, AT5G22690, AT5G42900, AT2G26650, AT1G70060, AT1G64060, AT1G17750, AT3G07770	[18, 67, 68]
Oxidation-reduction process	AT1G55670	[69, 70]
Protein located in mitochondria or chloroplast	AT1G55670, AT2G05100, AT3G08940, AT3G21055, AT1G67740, AT1G03130, AT2G45180, AT4G35770, AT4G01935, AT5G16930, AT2G34420, AT1G15820, AT2G34420, AT4G10340, AT1G61520, AT2G06520, AT3G27690, AT3G15190, AT1G77680, AT3G07770	[18, 63, 66, 70]
Regulation of cell cycle or differentiation	AT5G66570, AT2G26650, AT5G46070, AT2G42840	[18]
Transporter	AT1G55670, AT1G03130, AT2G45180, AT4G11670, AT5G66570, AT3G11964	[18]
Regulation of protein dephosphorylation or other modification	AT3G08940, AT3G21055, AT1G67740, AT1G03130, AT1G15820, AT5G12400, AT2G20850	[18]
Protein synthesis or proteolysis	AT3G15190, AT1G77680	
Nucleotide binding, regulation of transcription	AT3G08940, AT3G07650, AT5G66570, AT5G12400, AT2G42270, AT1G70060, AT2G40770, AT5G04290, AT1G33700, AT4G35240, AT1G14790	[18]
sn (o) RNA or other ncRNA	AT4G13495, AT5G09585	
ATP binding, ATPase or kinase activity	AT2G20850, AT2G42270, AT2G40770, AT1G17750	
Signaling transduction	AT5G22690, AT2G20850, AT5G13000, AT1G64060, AT1G17750	[18, 71]

^aSuggests the function of RNA itself, for example, rRNA, or the functions in its expressed proteins

^bThe functions of many transcripts were inferred by gene ontology (GO) analysis using the online tool in TAIR (<http://www.arabidopsis.org/>) and some functions were inferred from the recent publications

Table 7 Potential functions of the 41 transcripts presenting extensively higher m⁶A methylation in flowers than that in leaves and roots in *Arabidopsis* (fold change >10 or <0.1, FDR <10⁻¹⁰)

Potential functions ^a	Gene ID	References ^b
Transporter	AT1G15960, AT3G16460, AT1G80270, AT4G20860, AT3G23560, AT4G18197, AT5G44110, AT3G04620, AT4G39100	[72–75]
Defense or stress response	AT2G02100, AT1G27170, AT4G25720, AT3G16460, AT2G14080, AT4G39100, AT4G20860, AT3G23560, AT2G01830	[73, 76–78]
Redox process	AT3G50440, AT4G34900, AT2G07785, AT4G36530, AT4G20860	[18, 79]
Differentially or specifically expressed during flowering	AT3G23450, AT1G44890, AT5G44110, AT1G18370, AT1G05070, AT3G04620, AT5G62580, AT2G27380, AT2G45730, AT3G23560,	[18, 80–83]
Response to abscisic acid stimulus	AT1G76260	[84]
Cell proliferation, differentiation or circadian rhythm	AT1G78910, AT1G18370, AT1G19990, AT3G04620, AT5G62580, AT2G45730, AT5G66550, AT2G05440	[18, 80, 82]
Protein located in mitochondria or chloroplast	AT1G78910, AT4G25720, AT5G22608, AT1G80270, AT3G01200	[70, 85]
Nucleotide binding, regulation of transcription	AT1G80270, AT2G45730	
Protein synthesis, modification, or proteolysis	AT3G28500, AT3G27110, AT2G40205, AT2G23890, AT2G45730, AT1G07070, AT4G05040, AT2G01830, AT2G27900,	[18, 86, 87]
ATP binding, ATPase or kinase activity	AT3G01200, AT2G14080	
Signaling transduction	AT2G27900, AT2G14080, AT2G01830	[78, 88]
Carbohydrate metabolism or energy release	AT3G22210, AT1G22940, AT4G36530	[18]
sn (o) RNA or other ncRNA	AT3G57645	

^aSuggests the function of RNA itself, for example, rRNA, or the functions in its expressed proteins

^bThe functions of many transcripts were inferred by gene ontology (GO) analysis using the online tool in TAIR (<http://www.arabidopsis.org/>) and some functions were inferred from the recent publications

Table 8 Potential functions of the 23 transcripts presenting extensively higher m⁶A methylation in roots than that in leaves and flowers in *Arabidopsis*

Potential functions ^a	Gene ID	References ^b
Transporter	AT5G52050, AT4G27140, AT4G29030, AT4G28520	[18]
Nutrient reservoir activity	AT4G27140, AT1G03890, AT4G28520	[89] Gruis
Cell proliferation, differentiation or [AQ6]	AT2G36120, AT1G56660, AT4G34410, AT2G22860,	[81, 90, 91]
Defense or stress response	AT4G34410, AT5G07010, AT5G52050, AT2G05940, AT5G42380, AT4G28520	[18, 92–96]
Redox process	AT4G34410, AT1G18300, AT4G12960, AT2G34600	[97]
Carbohydrate metabolism	AT1G27440	[98]
Regulation of transcription	AT4G34410	
Protein located in mitochondria or amyloplast	AT1G18300	
Protein dephosphorylation or phosphorylation	AT1G48040, AT4G18250, AT5G42370	
Signaling transduction	AT4G34410, AT5G07010, AT2G05940, AT2G34600, AT4G18250, AT4G28520	[18, 99, 100]
Unknown protein	AT1G62080, AT1G62000, AT1G62333	

^aSuggests the function of RNA itself, for example, rRNA, or the functions in its expressed proteins

^bThe functions of many transcripts were inferred by gene ontology (GO) analysis using the online tool in TAIR (<http://www.arabidopsis.org/>) and some functions were inferred from the recent publications

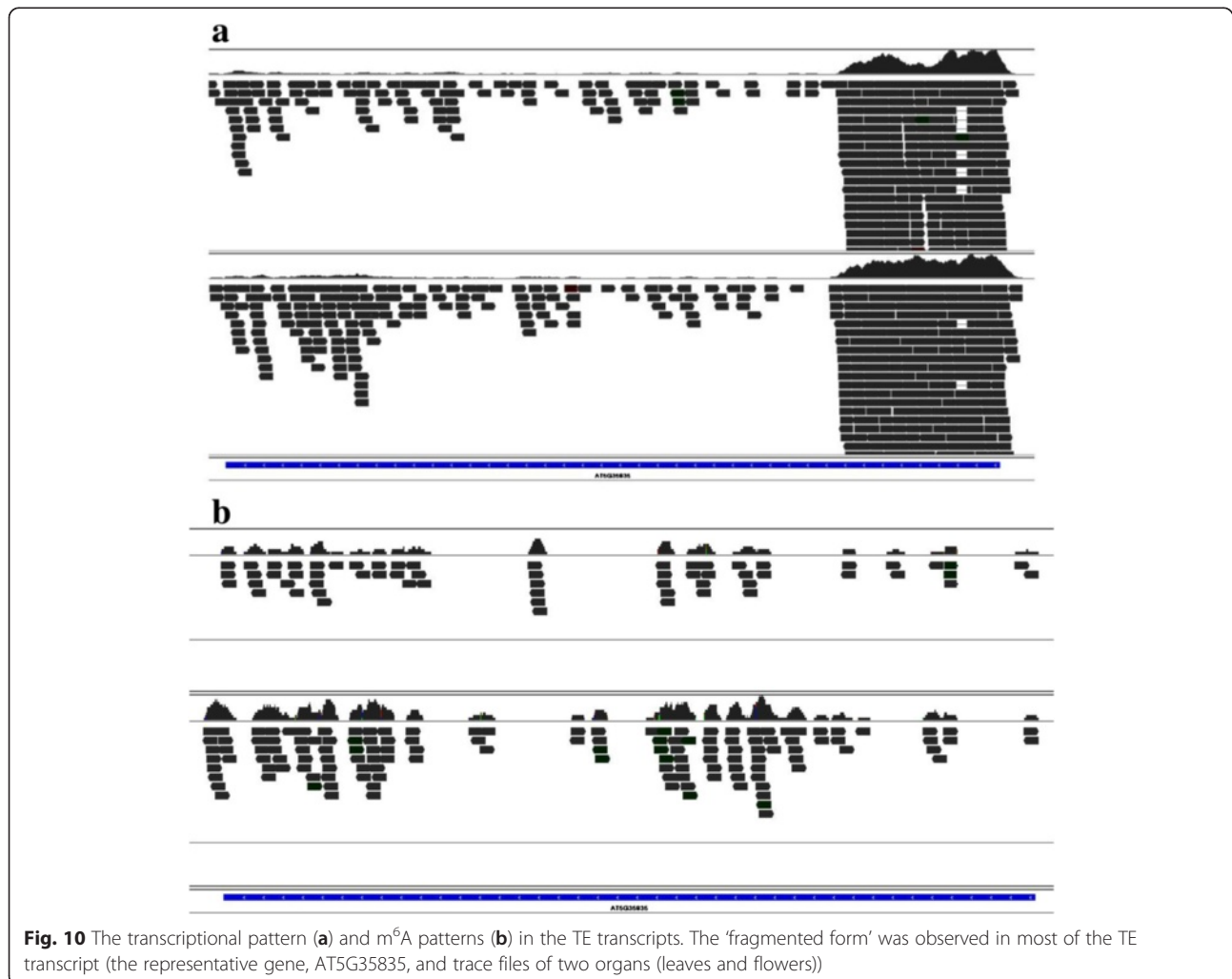


Fig. 10 The transcriptional pattern (a) and m⁶A patterns (b) in the TE transcripts. The 'fragmented form' was observed in most of the TE transcript (the representative gene, AT5G35835, and trace files of two organs (leaves and flowers))

(Fig. 10a). In some cases, the 5' region of TEs was highly transcribed, but the other regions were much less expressed (Fig. 10a). Therefore, most of the TE transcripts remained a 'fragmented' form in the cells with a relatively high m⁶A extent and a low transcript level.

Discussion

Improvement of biotechnology is prerequisite for successful m⁶A-seq

RNA isolation from plants is sometimes difficult due to a thick cell wall which may be difficult to disrupt during RNA extraction [101, 102]. In addition, plant cells also produce secondary molecules (for example, polysaccharides), which are collected during RNA precipitation and can be problematic for RNA purification [101]. We modified the CTAB protocol for RNA isolation. The improved buffer showed a potential to efficiently disrupt cell walls, and specifically precipitate RNA, thus a large quantity of high purity RNA from *Arabidopsis* was obtained for mRNA-seq, m⁶A-seq, and input RNA-seq in this study (Additional file 11).

Another significant improvement in this study is that we optimized the protocol for m⁶A RNA immunoprecipitation to improve RIP efficiency and to minimize non-specific precipitation. We found that procedures including pre-precipitation through adding beads and IP buffer in the RNA solution before adding m⁶A antibody to exclude any non-specific binding RNA, and a vigorously washing of the binding beads after incubation with m⁶A antibody three to four times using IP buffer can significantly reduce the background (non-specific precipitation) in the RIP experiment. Incubation of the beads binding with RIP RNA in the dilution buffer at 50 °C for 90 min facilitated washing down of m⁶A RNA from the beads to improve m⁶A RNA yield.

m⁶A patterns between plant and mammal

The m⁶A patterns between plant (Figs. 4a and 5) and mammal were similar, for example, both rich near stop codons and 3'UTR [6, 8, 12, 13]. Both kingdoms had a similar consensus m⁶A methylation motif 'RRm⁶ACH' and a close frequency of m⁶A site per transcript in the transcriptome [6, 12, 13]. These phenomena indicated that m⁶A RNA methylation may be conserved between plant and mammal.

Some differences, however, were found between *Arabidopsis* and mammals as aforementioned (for example, Fig. 3a). These differences more likely represented the different m⁶A methylation extent and unique patterns between two species, or may result from the distinct depths of m⁶A-seq between two studies. Resolution in the m⁶A-seq with a low depth in the previous studies may be insufficient to discern the weak m⁶A signals in the coding regions in most of mRNA (Figs. 4a and 5).

The previous report also suggested under-estimation of m⁶A sites in their studies [6, 8].

Dominant m⁶A enrichment in 5'UTR in *Arabidopsis* was reported by Luo *et al.* [13]. However, both our study from six *Arabidopsis* m⁶A-seq datasets (Fig. 5) and a recent report from rice m⁶A-seq of two different tissues [12] did not observe this dominant m⁶A pattern as the authors claimed a unique m⁶A pattern in the plant in their paper [13]. The m⁶A modified motif was confirmed by numerous studies highly conserved among the eukaryotes, including between two kingdoms of plant and animal [2, 6–8, 103]. A number of studies did not observe the dominant m⁶A enrichment in 5'UTR in mammals either [6, 8, 11]. The dominant m⁶A near the start codon reported by Luo *et al.* [13] may be an experimental artifact, for example probably caused by contamination from mRNA as a dominant peak was also found near the start codon in the overall pattern of mRNA-seq (Fig. 5). Nevertheless the difference in m⁶A enrichment pattern needs further confirmation.

The proportion of the m⁶A modified transcripts (over two-third) estimated in this study is relatively much higher than the previously reported [6, 12]. The previous studies with the robust experiments confirmed that the m⁶A modification is required for RNA stability and RNA transport from nucleus to cytoplasm [4, 6]. Otherwise, RNA will be degraded in the cells [3, 4, 6]. This suggested that the major proportion of mRNA in the cells, for example, over 70 % as estimated in our study, may rationally be modified by m⁶A [3]. Therefore, our estimation may reflect the genuine phenomenon in the cells.

Extensively high m⁶A methylation in certain transcripts may be suitable or required for the biological functions of these transcripts

Eukaryotic cells are highly compartmentalized and functionally differentiated [104–106]. mRNA translated into proteins for energy carriers (for example, ATP or GTP), transporter (for example, ion transporter), stress response, redox, protein post-translational modification, and protein located in mitochondria or chloroplast were found highly methylated by m⁶A in this study (Table 3). The common feature of these proteins was that they were a direct transporter for energy molecules, for example, ATP or GTP, or accomplishment of their biological functions was dependent on these energy chaperones [106, 107]. These transcripts may be transported for their protein translation near compartments for energy metabolism in the cells (for example, near mitochondria or chloroplast) or in the cells which were highly differentiated for energy process or stress response [109–111]. A long evolutionary history of m⁶A modification may imprint these transcripts with extensively high m⁶A methylation for their molecule stability [4, 112].

Extensive high m⁶A methylation was also found in the transcripts for some signaling factors, regulation factors (for example, regulation of DNA replication, RNA transcript, and protein synthesis and post-transcriptional process) and in certain sn(o)RNA (Table 3). These transcripts were highly or delicately regulated to maintain a low TL in the cells in most cases [107, 108, 113]. High methylation in these transcripts may endow RNA stability to these transcripts with a low TL, or confer signaling recognition to these transcripts [1, 3, 6, 112].

The transcripts of certain pseudogenes were extensively modified by m⁶A (Table 3). Accordingly, the transcripts of their relative functional genes had high methylation, for example, gene for NADH dehydrogenase ('AT2G07709') (Table 3). m⁶A modification proved a highly selective and regulative event [6, 8, 112]. If the transcript of a parent functional gene was extensively methylated by a regulative system, the transcript of the relative pseudogene may also be highly methylated by the same regulative system.

Dysfunction of m⁶A modification in the human cells resulted in an abnormal circadian rhythm [11]. Several transcripts responsible for regulation of circadian rhythm were highly methylated by m⁶A in *Arabidopsis* (Tables 3 and 7), suggesting that m⁶A may also play an important role in regulation of circadian rhythm in plants.

The m⁶A topological patterns and their potential functions in different types of RNAs

A frequency of 15 consensus (RRm⁶ACH) sequences per transcript should occur in the transcriptome [2, 14]. In deed, the occurrence of m⁶A methylation in the transcriptome was much lower than this expected frequency [2, 6, 114], suggesting that the majority of the consensus sequences were either not modified or many of them were demethylated promptly after the accomplishment of the biological metabolisms due to m⁶A modification [2]. As a result, methylation and demethylation may maintain a dynamic oscillation in the cells in response to environmental stimuli [2, 115, 116].

The extensively lower m⁶A signals in the coding regions including the splicing sites in most of mRNA discovered in this study (Figs. 4a and 5) could come from the sequencing bias. But the technical bias resulting in a large number (over 70 %) of the m⁶A modified mRNA containing this feature is impossible (Fig. 4a). The m⁶A methylation is required for a correct RNA splicing event [6, 116, 117]. Nevertheless, the most possible reason for the low signal detected in the coding regions in most of mRNA in this study may result from a prompt m⁶A demethylation event after accomplishment of the RNA splicing event [115, 116]. The consequent m⁶A demethylation in the coding regions may facilitate a speed of movement of ribosomes through mRNA chain thus may confer a high efficiency protein

synthesis, while reservation of a great higher extent of methylation at the stop codon or 3'UTR may be responsible for RNA stability, signaling for transport and translocation, or as regulatory elements for protein translation through the recruitment of specific factors onto these m⁶A sites for RNA transport or protein synthesis [4, 112, 118, 119].

Dominant m⁶A enrichment near stop codons and 3' UTR (as shown in Fig. 4a) was observed in most (over 70 %) of mRNA in this study as previously reported [6, 8, 12, 13]. This m⁶A distributing type (Fig. 4a) may represent the typical m⁶A topological pattern in most of the mature mRNA. However, a small proportion of mRNA did not present this m⁶A enrichment in 3'UTR (as shown in Fig. 4b). m⁶A methylation confers RNA stability [4]. Non-dominant m⁶A enrichment in 3'UTR in this small proportion of mRNA may reflect a phenomenon of 'subsequent-demethylation' to the m⁶A dominant peaks in 3'UTR or stop condon, further suggesting that these RNA may undergo a process of degradation due to m⁶A demethylation [4]. Therefore, different m⁶A topological patterns in mRNA may reflect RNA status or fate in the cells, for example, pre-mature RNA, mature RNA, or RNA being in degradation.

Both rRNA and tRNA were mainly modified by numerous types of cytosine methylation [1, 3]. However, a relatively high m⁶A methylation was found in all rRNAs (Fig. 6a and b) and in a certain proportion of tRNAs (approximately 10 %) (Fig. 6c) in *Arabidopsis* in this study. Mature rRNA and tRNA were derived from pre-rRNA and pre-tRNA through a series of complex biological and molecular processes, including splicing and folding. The splicing machinery in rRNA and tRNA was similar to that in mRNA in eukaryotes [3]. m⁶A may guide a correct splicing event in these types of RNAs as the role of the m⁶A methylation required for the correct splicing events in mRNA [6]. m⁶A may not undergo a subsequent demethylation event after splicing for the mature rRNA, but demethylation of m⁶A after splicing may be required for the mature tRNA as hypothetically aforementioned for most of mRNA. This would be the reason that m⁶A methylation was reserved and observed in all rRNAs (Fig. 6a and b), but it was detected in a small proportion of tRNAs (Fig. 6c).

Therefore, diverse m⁶A patterns and topologies may be unique or required for the miscellaneous functions in the different types of RNAs [3, 112].

Potential roles of differential m⁶A methylation among plant organs

Differential gene expression among plant organs has proved responsible for organ differentiation and development [120, 121]. Differential level of m⁶A methylation among three organs was much higher than that in

gene transcript level (Table 4), suggesting that m⁶A modification may be another important contributor for organ differentiation or maintenance of differential status among the organs in *Arabidopsis*.

The transcripts presenting extensively higher m⁶A modification in an organ than other organs showed a connection of the functions of these transcripts required for or specific to this organ. For example, the transcripts presenting an extensively higher level of m⁶A methylation in leaves were related to photosynthesis metabolism or proteins located in mitochondria or chloroplast, and those in roots showed response to stresses, redox process, and transporters (Tables 6 and 8). However, most of the differential and extensively methylated transcripts in flowers were related to regulation of reproductive organ development, stress response, cell proliferation, differentiation, or circadian rhythm (Table 7) [18, 122]. Dysfunction of *METTL3*, the gene responsible for m⁶A modification, can result in an arrest of the early development in embryo at the globular stage in *Arabidopsis* [7], suggesting that m⁶A methylation may play an important role in differentiation and development of the reproductive organs in plants.

The proportion of the m⁶A modified transcripts was the highest in the roots among three organs (Additional file 3). The surrounding environment for root growth is more complex than that for leaves and flowers [123, 124], which may require a higher proportion of the m⁶A transcripts in roots to adapt to more diverse conditions [2–4]. However, the overall extent for m⁶A RNA methylation showed the highest in the leaves among three organs (Table 1). The leaves are the major organ in plants responsible for photosynthesis metabolism and energy transition [123]. This may require a higher extent of m⁶A RNA methylation in the leaves to fit for these metabolisms that were processed in severe conditions in most of cases if our hypothesis aforementioned is rational.

Potential biological significance of gene transcript and m⁶A patterns in TE

Most of the TE transcripts (>85 % in this study) remained a relatively low level in the cells. This may repress a neo-transposition of TEs into the genome [125]. 17 % to 85 % of the genomic sequences are composed of TE in the higher plant species [126, 127]. In most of cases, the neo-transposition of TEs was highly repressed because it is often detrimental to the host due to a prompt expansion of the genomic size or dysfunction of the functional genes by this event [128]. The fragmented TE transcripts may not be reversely transcribed into a complete cDNA, thus the malignant TE transposition may be consequently avoided. In addition, the distribution of these unconnected transcripts in the cells may play a role similar to the small interfering

RNA (siRNA), which may in turn repress the transcription or the neo-transposition of these TEs [125, 129]. The remnant TE transcript fragments may also be induced in response to stress, which may further trigger a serial of complex reactions [127]. Some of the fragmented TE transcripts may play a role as ‘a regulator’ for other gene expression or as a direct regulator for the nearby genes [125, 127, 130, 131], or may work as powerful regulators of the immune response as the functions recently discovered in some miRNA [132]. Because the fragmented transcripts were more likely to be degraded than the intact transcripts [3], relatively high m⁶A methylation in the fragmented TE transcripts may prevent these segmented transcripts from further degradation so that a relatively low level of these transcripts can be maintained in the cells [3].

Conclusions

Thanks to significant improvements of technologies for RIP experiments in this study, high resolution of transcriptome-wide mapping of m⁶A was available in *Arabidopsis*. This is the first study for comprehensive characterization of m⁶A patterns of different types of RNAs, relationship between m⁶A methylation extent and gene transcript level, and differential features of m⁶A methylation among three plant organs. Two-third of the transcripts were modified by m⁶A in *Arabidopsis*. 35,000 to 48,000 m⁶A sites and approximately 1.4 to 2.0 m⁶A sites per transcript were mapped to the *Arabidopsis* genome.

Over 85 % of the m⁶A modified transcripts had a relatively high m⁶A methylation level ($P < 0.05$), while <4 % had a low m⁶A extent compared with their transcript level ($P < 0.05$). Approximately 5.5 % of the methylated transcripts presented extensively high methylation (fold change >10 compared to TL, and FDR <10⁻¹²). The highly expressed transcripts were relatively less methylated by m⁶A and *vice versa* ($P < 0.001$). The 290 (2.1 %) highly methylated transcripts were mainly expressed for stress response, redox, signaling factors, regulation factors, and some ncRNA. Most of the biological functions in these transcripts were involved in molecule binding, transferase, transporter, and kinase activity.

Most of mRNA (over 70 %) was characterized by a typical m⁶A topology, that is, one or two predominant peaks at the stop codon or 3'UTR accompanying with extensively low m⁶A signals in the coding regions. Unlike a recent observation of another predominant m⁶A enrichment in the 5' mRNA in *Arabidopsis* [13], we found that m⁶A predominantly distributed only at the stop codon or 3'UTR. Some sn(o) RNAs were also highly methylated with a single m⁶A site in these transcripts. All rRNAs was relatively highly methylated by one or several m⁶A sites. Non- or slight-m⁶A methylation was observed in most of

tRNAs (approximately 90 %), and the remaining tRNAs were relatively hyper-methylated by a single m⁶A site. Interestingly, most (over 75 %) of the transcribed TEs maintained a relatively high m⁶A methylation. Therefore, the topologies of m⁶A in different RNAs not only confer diverse m⁶A patterns in the cell, the unique m⁶A pattern in a specific RNA may endow special functions to this RNA.

The similar m⁶A patterns between plant and mammal suggested that m⁶A methylation may be conserved between two living kingdoms. Differences were also found between plant and mammal, which may represent their unique m⁶A patterns in the two living kingdoms.

Proportion of transcripts (33.5 %) showing differential m⁶A methylation among three organs was greatly higher than that (22.6 %) presenting differential transcript level in *Arabidopsis* ($P < 0.00035$). Function of the transcripts with extensively higher methylation in an organ than others were required or suitable for unique biological roles of this organ. Therefore, m⁶A methylation may be an important contributor to the organ differentiation and may confer unique functions to this organ.

Methods

Plant materials

Wild type, Columbia ecotype (Col-0), of the mouse ear cress (*Arabidopsis thaliana*) was used in this study. The plants were grown in the greenhouse under a photoperiod of 16 h light/8 h dark at 22–24 °C. When the plants were at the blooming period (5 weeks after seed germination), the plant materials of the flowers, rosette leaves, and roots were separately collected, treated with liquid nitrogen and stored at –80 °C until use.

RNA isolation and purification

All centrifuge tubes and pipette-tips are RNase-free or must be treated with DEPC. All buffers were RNase free or prepared using DEPC-treated dd H₂O. The modified CTAB buffer was used for RNA isolation [133]. In brief, approximately 10 g of the frozen plant materials were ground into fine powder in liquid nitrogen. The plant powder was promptly transferred into four 50 mL tubes with 25 mL CTAB buffer (2 % CTAB, 1.0 % PVP-40, 2.0 M NaCl, 100 mM Tris, 25 mM EDTA-Na₂, and 1.0 % β-mercaptoethanol) in each tube. Incubate the tubes at 65 °C for 10 min and invert tubes for several seconds every minute during incubation. Add 200 μL chloroform to each tube, invert quickly 150–200 times. Centrifuge tubes at 4,500 g for 2 min at 4 °C, and discard most of the chloroform solution using a pipette-tip. Centrifuge tubes at 15,000 g for 5 min at 4 °C. Transfer the supernatant to new tubes. Add 8.0 mL LiCl (8.0 M) into each tube and mix well. Store the mixture at –20 °C for 30 min, then centrifuge at 17,000 g for 30 min at 4 °C.

Use 2 mL 80 % ethanol to rinse RNA pellet. Centrifuge at 17,000 g for 2 min, discard the ethanol, and then dry tubes in the laminar-flow hood. Dissolve the dried RNA pellet using 400 μL RNase-free water and treat with DNase (Promega, Madison, WI, USA) to remove DNA contamination. Add 300 μL chloroform-phenol (1:1, v/v) into the tube, invert quickly 200 times. Centrifuge tubes at 13,000 g for 1 min at 4 °C, and discard most of the chloroform-phenol solution in the hood. Centrifuge tubes at 15,000 g for 5 min at 4 °C. Transfer the supernatant to new tubes. Add 2.8 volume of ethanol and 0.10–0.15 volume of NaAc (pH 5.6), and mix well. Store the mixture at –20 °C for 30 min, then centrifuge at 15,000 g for 30 min at 4 °C. Store the RNA pellet in the ethanol-NaAc solution at –80 °C until use.

RNA fragmentation

The purified total RNA was diluted in the fragmentation buffer (10 mM ZnCl₂ and 10 mM Tris-HCl, pH 7) with the RNA final concentration of approximately 1.0 μg μL⁻¹ [6, 10]. The diluted RNA was fragmented into approximately 100-nucleotide-long by incubation at 95 °C for 5 min. The chemical fragmentation reaction was stopped with 0.05 M EDTA. The ethanol-NaAc solution was used to precipitate RNA. The fragmented RNA was prepared for RIP and m⁶A-seq.

RNA immunoprecipitation (RIP)

Approximately 2.5 mg fragmented total RNA was resuspended in the 1,000 μL IP buffer (150 mM NaCl, 0.1 % NP-40, 10 mM Tris-HCl, pH 7.4, 2 mM RVC (Sigma-Aldrich, St. Louis, MO, USA), 200 U RNasin (Promega, Madison, WI, USA), and 0.5 mg mL⁻¹ BSA). Non-specific binding RNA was pre-precipitated by adding 3.0 μL Protein A bead (Life Technology, Grand Island, NY, USA) and incubation on a rotating wheel for 2 h. The magnet rack was used to precipitate the beads. The supernatant was transferred to a new tube. Add 5.0 μg m⁶A-specific monoclonal antibody (Merck Millipore, Billerica, MA, USA) into the tube containing RNA and IP buffer, and incubate on a rotating wheel for 3–4 h. Then add 5.0 μL Protein A bead (Life Technology, Grand Island, NY, USA) for an additional rotation for 2 h. The magnet rack was used to precipitate the beads. The beads were vigorously washed using 1,000 μL IP buffer three to four times. Discard the IP buffer. Add 300 μL dilution buffer (10 mM Tris-HCl pH 7.5) into the bead tube and incubate at 50 °C for 90 min. Precipitate the beads using the magnet rack and transfer the supernatant to a new tube. The ethanol-NaAc solution and glycogen were used to precipitate m⁶A RNA. The m⁶A RNA pellet was washed using 80 % ethanol and then resuspended into 15 μL dd-H₂O for m⁶A-seq and HPLC-MS/MS analysis.

mRNA-seq, m⁶A-seq, and RNA-seq from the input samples

The quality control (QC) tests for the RNA samples were performed using Agilent Technologies (Santa Clara, CA, USA). Library for mRNA-seq was generated using mRNA sequencing kit plus random primers. High throughput m⁶A-seq, mRNA-seq, and input RNA-seq of three samples of leaves, flowers, and roots was performed on HiSeq 2000 (Illumina Inc., San Diego, CA, USA) at Purdue University Genomics Core Facility (<http://www.genomics.purdue.edu/services/core.shtml>).

Approximately 10.0 µg purified total RNA was reserved for mRNA-seq before the RNA samples were used for fragmentation. And approximately 2.5 µg fragmented total RNA was reserved and used for the input RNA-seq before the RIP experiments. Thus, mRNA-seq, m⁶A-seq, and input RNA-seq were parallel and their data were mutually comparable in this study [6]. RNA integrity number (RIN) was estimated using a Nanodrop 2000 UV vis (Thermo Fisher Scientific, Wilmington, NC, USA). The QC tests were done by Agilent Technologies (Santa Clara, CA, USA). All RNA sequencing of three samples of leaves, flowers, and roots was performed on the same sequencer at the same batch.

HPLC-MS/MS

A total of 100–200 ng of input total RNA or m⁶A RNA from RIP experiment was digested by 2 U nuclease P1 (US Biological Life Science, Salem, MA, USA) at 37 °C for 2 h, and 0.5 U alkaline phosphatase (Promega, Madison, WI, USA) at 37 °C for an additional 2 h. A total of 5 µL of the digested and purified solutions were assayed by HPLC-MS/MS. Nucleosides were separated by reversed-phase high performance liquid chromatography, using a Waters Xterra C18 column (2.1 × 150 mm, 3.5 µm) with a water/acetonitrile gradient. Mass spectrometry was performed using an Agilent 6460 triple quadrupole mass spectrometer in positive electrospray ionization mode. Mass transitions were 268.1 → 136.1 for A and 282.1 → 150.1 for m⁶A (Additional file 2).

Alignment of reads and visualization of m⁶A peaks

Both RNA-seq and m⁶A-seq datasets were mapped to the *Arabidopsis* genome (TAIR10) using TopHat2 with a parameter of '-b2-fast' [134]. The potential PCR duplicates were removed by the parameter 'rmdup' rooted in SAMtools [135]. The fragment numbers for each transcript were estimated using the featureCounts with a parameter of '-p' [136].

The peaks and distributing patterns of m⁶A in the *Arabidopsis* transcriptome were visualized using free software, Integrative Genomics Viewer (IGV2.3, Boston, MA, USA [137]).

We tried several previously published protocols, for example, moving-window, to call m⁶A peaks based on comparison of m⁶A-seq with input RNA-seq counterpart. And we found all of these methods failed recognition of most (>92 %) of m⁶A sites in CDS (Additional file 12). We finally did not apply these methods in this study. Because of the extensively low non-specific immunoprecipitation rate (<1 %) in this study (Additional file 2), all the mapped reads in the m⁶A-seq were considered to be sequenced and derived from the specific immunoprecipitation of the m⁶A RNA fragments. Thus, an estimation of m⁶A peak number of a m⁶A modified transcript was calculated by this formula: total mapped absolute length covered by m⁶A fragments within the transcript/150, considered that library construction for m⁶A-seq was created from a m⁶A RNA pool with an average RNA length of approximately 106 nucleotides (Additional file 11: Fig. S3b) and average coverage of a peak in the m⁶A-seq data base was approximately 150-nucleotide long in this study as visualized by IGV 2.3.

Discernment of m⁶A topological patterns

Distribution of m⁶A sites in the different regions of the transcripts was estimated by Dominissini *et al.*'s method [6]. The consensus m⁶A motif sequences were figured out by Luo *et al.*'s protocol [13] with modification: approximately 1,000 the highest m⁶A peaks and approximately 100 nt length around each m⁶A peak were used for deduction of the consensus m⁶A motif sequences. The typical m⁶A patterns of different types of RNA were drawn from the m⁶A mapping analysis based on visualization using the IGV2.3 program [13].

The overall m⁶A distributing patterns were discerned by this method: a gene was splitted in to 60 bins. The read depth of each bin was normalized by per 1 kb per 1 Mb data, then the normalized depth was used to plot the patterns.

Comparison of m⁶A methylation extent versus transcript level

The sequenced fragment number of each transcript in mRNA-seq was normalized using the algorithm of Fragments Per Kilobase of Transcript Per Million Fragments Mapped (FPKM = Counts of mapped fragments × 10⁹) / (Length of transcript × Total count of the mapped fragments); 'fragment' refers to mapped reads after removal of PCR duplicates [138]. While the sequenced fragment number of each transcript in m⁶A-seq was normalized using a modified FPKM (MFPKM = Counts of mapped fragments × 10⁹) / (Total absolute mapped length on the chromosome covered by m⁶A fragments within the transcript × Total count of the mapped m⁶A fragments)), considered that the library in m⁶A-seq was derived only

from RNA fragments containing m⁶A sites, and not from the entire transcript [138].

The m⁶A methylation extent of a transcript were categorized into three groupings based on comparison of MFPKM of the transcript in the m⁶A-seq with the FPKM of the same transcript in the mRNA-seq using χ^2 test: (1) m⁶A methylation extent 'equivalent' to transcript level ('equivalent', ratio of FPKM to MFPKM fits 1:1 ($P < 0.05$)); (2) methylation extent higher than transcript level ('Hi', ratio of FPKM to MFPKM < 1 ($P < 0.05$)); and (3) methylation extent lower than transcript level ('Low', ratio of FPKM to MFPKM > 1 ($P < 0.05$)). The chi-square value was determined by this formula: $\chi^2 = (MFPKM * 100 / (MFPKM + FPKM) - 50)^2 / 50 + (FPKM * 100 / (MFPKM + FPKM) - 50)^2 / 50$.

Analysis of both differential transcript level and differential m⁶A methylation among plant organs

mRNA-seq data were normalized by FPKM as described above. χ^2 tests were used to estimate whether FPKM was significantly different between two organs using R 3.1 (<http://cran.r-project.org/bin/windows/base/>). The transcripts with fold change in FPKM > 2.0 or < 0.5 , and FDR < 0.02 were considered differentially expressed between two organs [6, 10].

To minimize influence of transcript level on estimation of differentiation of m⁶A extent, m⁶A-seq data were normalized by a specific algorithm, NFPKM (NFPKM = MFPKM in m⁶A-seq / LOG (FPKM in mRNA-seq, 2)). χ^2 tests were also used to estimate whether NFPKM of a m⁶A modified transcript was significantly different between two organs using R 3.1. The transcripts with fold change of NFPKM > 2.0 or < 0.5 , and FDR < 0.005 were considered differentially methylated between two organs [6, 10]. The transcripts commonly presenting higher m⁶A extent in an organ in the two replicates were used for gene ontology (GO) analysis. P values of the chi-square tests to all gene transcripts of a replicate were input in R 3.1.2 ('Pumpkin Helmet') to estimate FDR of each transcript under a parameter of 'p.adjust (P value, method = 'fdr')'. The fold change is a fixed threshold for all classifications, thus FDR thresholds may vary with different analyses.

Visualization of the overall differential patterns

The overall patterns of differential transcript level of all transcripts were discerned using ratio of FPKM of mRNA-seq between two organs. Similarly, the overall patterns of differential m⁶A methylation of all transcripts were depicted using ratio of NFPKM derived from both m⁶A-seq and mRNA-seq (see above) between two organs. The heatmap representing the overall differential patterns of gene transcript and m⁶A methylation was created using R3.1 (<http://cran.r-project.org/bin/windows/base/>).

GO and KEGG pathway analysis

The GO results and potential molecular functions in the transcripts were deducted from the online tool released in the TAIR website (<http://www.arabidopsis.org/>) [139]. And molecular functions in some transcripts were inferred from the recent publications.

The Kyoto Encyclopedia of Genes and Genomes (KEGG) pathways in certain transcripts of interests were figured out using the online tool released in the DAVID bioinformatics resources (<http://david.abcc.ncifcrf.gov/>).

qRT-PCR

Quantitative real-time PCR (qRT-PCR) was performed to assess the relative abundance of m⁶A RNA in the RIP samples. All purified RNA templates were transferred into cDNA using Quanta qScript™ cDNA Synthesis Kits (Quanta BioSciences, Inc., Gaithersburg, MD, USA). Eleven genes were randomly chosen for this test (Additional file 9). The qRT-PCR primers were designed to span exon-exon junctions in order to eliminate the potential amplification of genomic DNA and non-spliced mRNA. qRT-PCR was performed on C1000 Thermal Cycler (Bio-RAD) using SYBR Green SuperMix buffer (Bio-RAD) and 300 ng total cDNA template for amplification. Because the qRT-PCR amplicon spanned an exon-exon junction with a length of 80–150 bp and the m⁶A enrichment in the region around splicing sites was usually low in most of mRNA in this study (Fig. 4a), cDNA from total RNA of the *Actin2* gene was used for housekeeping gene to estimate the relative abundance (RA) of m⁶A RNA in the qRT-PCR amplicons based on this algorithm: $RA = 100 \times 2^{-\Delta C}$. The expected abundance (EA) of m⁶A RNA in the m⁶A-seq dataset was estimated by this algorithm: $EA = 100 \times$ (the mapped m⁶A RNA reads of the test gene in m⁶A-seq and in the region for qRT-PCR test / the mapped RNA reads of the *Actin2* gene in mRNA-seq and in the region for qRT-PCR test). The consistency between the AR and ER patterns among three organs was compared (Additional file 10).

Ethics statement

The plant materials used in this study are freely used and available to all researchers without any protection for intellectual property right. This research meets all applicable standards for the ethics of experimentation and research integrity from all five institutes that provide supports to this study.

Data access

The data discussed in this publication have been deposited in NCBI's Gene Expression Omnibus and are accessible through GEO Series accession number GSE72706.

Additional files

Additional file 1: Table S1. The sequenced and mapped reads in the m⁶A-seq, mRNA-seq, and input RNA-seq samples. (DOC 43 kb)

Additional file 2: Figure S1. The m⁶A peak and adenosine peak deduced from the HPLC-MS/MS analysis. **a** The relative m⁶A peak height (upper) and adenosine peak height (lower) in the standard sample. **b** The relative m⁶A peak height (upper) and adenosine peak height (lower) in the input sample. **c** The relative m⁶A peak height (upper) and adenosine peak height (lower) in the RIP sample. (DOC 50 kb)

Additional file 3: Table S2. Number of transcripts in the mRNA-seq and the m⁶A-seq (RIP) samples and proportion of the m⁶A modified transcripts in the three organs of *Arabidopsis*. (DOC 33 kb)

Additional file 4: Table S3. Number of m⁶A sites detected in the three organs of *Arabidopsis*. (DOC 37 kb)

Additional file 5: Table S4. Ratio of m⁶A/A in the three organs of *Arabidopsis*. (DOC 38 kb)

Additional file 6: Table S5. Category of the m⁶A modified transcripts based on the number of m⁶A sites per transcript. (DOC 37 kb)

Additional file 7: Table S6. Proportion of two types of m⁶A distributing feature in mRNA. (DOC 30 kb)

Additional file 8: Table S7. The transcriptome-wide normalized read depth in the 60 bins of the gene representing the overall m⁶A patterns in the different regions of the genes. Non-significant differences were found between three organs ($P = 0.761$). (DOC 108 kb)

Additional file 9: Table S8. The primers used for qRT-PCR. (DOC 35 kb)

Additional file 10: Figure S2. The relative abundance (RA) of m⁶A RNA deduced from qRT-PCR and the expected abundance (EA) of m⁶A RNA deduced from the m⁶A-seq dataset. **a** RA for 'AT1G35710', **b** EA for 'AT1G35710', **c** RA for 'AT3G07610', **d** EA for 'AT3G07610', **e** RA for 'AT4G14410', **f** EA for 'AT4G14410', **g** RA for 'AT2G28490', **h** EA for 'AT2G28490', **i** RA for 'AT1G03880', **j** RA for 'AT1G03880', **k** RA for 'AT1G33700', **l** EA for 'AT1G33700', **m** RA for 'AT2G07836', **n** EA for 'AT2G07836', **o** RA for 'AT5G20960', **p** EA for 'AT5G20960', **q** RA for 'AT5G22700', **r** EA for 'AT5G22700', **s** RA for 'AT3G13400', **t** EA for 'AT3G13400', **u** EA for 'AT4G38120', **v** EA for 'AT4G38120'. (DOC 1342 kb)

Additional file 11: Figure S3. RNA QC results of the total RNA and the RIP RNA for m⁶A-seq samples. **a** RNA quality for the total RNA sample was high with RIN over 8.5. **b** RNA fragmentation for the m⁶A-seq samples was consistent in the experiments, with an average length of 106 nt. (DOC 313 kb)

Additional file 12: Spreadsheet files show the m⁶A peaks detected in three organs using 'Moving-window' program and their positions in the genome. (ZIP 547 kb)

Abbreviations

ATP: adenosine triphosphate; BSA: bovine serum albumin; cDNA: complementary DNA; CDS: coding sequence; CI: confidence intervals; CTAB: cetyl trimethylammonium bromide; DEPC: diethylpyrocarbonate; EA: expected abundance; EDTA: ethylenediaminetetraacetic acid; FDR: false discovery rate; FPKM: fragments per kilobase of transcript per million fragments mapped of the transcript in mRNA-seq; GO: gene ontology; GTP: guanosine triphosphate; HPLC: High-performance liquid chromatography; KEGG: the Kyoto Encyclopedia of Genes and Genomes; m⁶A: N⁶-methyladenosine; m⁶A-seq: RNA sequencing based on m⁶A RNA immunoprecipitation; MFPKM: modified fragments per kilobase of transcript per million fragments mapped of the transcript in m⁶A-seq; mRNA-seq: RNA sequencing from oligo-dT RNA; MS: mass spectrometry; NADH: nicotinamide adenine dinucleotide; NFPKM: MFPKM in m⁶A-seq divided by LOG (FPKM in mRNA-seq, 2); PVP: polyvinylpyrrolidone; QC: quality control test; qRT-PCR: quantitative real-time polymerase chain reaction; RA: relative abundance; RIN: RNA integrity number; RIP: RNA immunoprecipitation; sn(o)RNA: small nuclear RNA and small nucleolar RNA; TAIR: the *Arabidopsis* Information Resource (<https://www.arabidopsis.org/>); TE: transposable element gene; TL: transcript level; Tris: tris(hydroxymethyl)aminomethane; TSS: transcription start site; U: unit; UTR: untranslated region.

Competing interests

The authors declare that they have no competing interests.

Authors' contributions

YW, KT, and XZ conceived and designed the experiment. YW grew *Arabidopsis* plants and collected the plant materials. YW and DZ performed the RNA extractions. YW carried out the m⁶A RNA IP experiment. KT and SX performed the mapping analysis. YW, KT, and SX designed the algorithm for analysis of m⁶A differential patterns among organs, and carried out analyses of m⁶A patterns, differential gene transcripts, and differential m⁶A methylation among organs. DZ and ZW participated in some statistical analyses. YW carried out qRT-PCR. YW and DZ analyzed the data. YW drafted the manuscript, SX, ZL, KT, ZW, and XZ provided critical comments. All authors read and approved the final manuscript.

Acknowledgments

This work was completed in Prof. Jian-kang Zhu's lab. We highly appreciate Prof. Jian-kang-Zhu for his strong supports to this project including financial support for all experiments and experts in his group for analysis of a large number of datasets, and his valuable suggestions for improvement of the manuscript and correction of some scientific conceptions in the draft. We thank Xingang Wang and Huiming Zhang for providing valuable suggestions on improvement of RIP experiments in this study, and Rebecca Ann Stevenson for her valuable work on English polishing of the manuscript, to Prof. Renyi Liu and Yangqiang Li for their estimation of m⁶A peaks using the Moving-window program. This work was funded by the 2012 Shaanxi Province Fund for Returnees Scientists from Foreign Study (A289021201), Chinese Academy of Sciences, China Scholarship Council Project (22861057), USA NIH grants (R01GM070795 and R01GM059138) to Professor Jian-kang Zhu, and National Science Foundation of China (31101166).

Author details

¹State Key Lab Laboratory of Crop Stress Biology for Arid Areas, College of Horticulture, College of Life Sciences, Northwest A&F University, Yangling, Shaanxi 712100, China. ²Department of Horticulture and Landscape Architecture, Purdue University, West Lafayette, IN 47907, USA. ³Shanghai Center for Plant Stress Biology, Shanghai Institutes for Biological Sciences, Chinese Academy of Sciences, Shanghai 200032, China. ⁴Institute of Biotechnology, Jiangsu Academy of Agricultural Sciences, Nanjing 210014, China. ⁵College of Bioscience and Biotechnology, Yangzhou University, Yangzhou 225009, China.

Received: 25 October 2015 Accepted: 18 November 2015

Published: 14 December 2015

References

- Matera AG, Terns RM, Terns MP. Non-coding RNAs: lessons from the small nuclear and small nucleolar RNAs. *Nat Rev Mol Cell Biol.* 2007;8:209–20.
- Pan T. N⁶-methyl-adenosine modification in messenger and long non-coding RNA. *Trends Biochem Sci.* 2013;4:204–9.
- Grosjean H. Fine-tuning of RNA functions by modification and editing. Berlin: Springer-Verlag; 2005.
- Wang X, Lu Z, Gomez A, Hon GC, Yue Y, Han D, et al. N⁶-methyladenosine-dependent regulation of messenger RNA stability. *Nature.* 2013;7481:117–20.
- Bodi Z, Bottley A, Archer N, May ST, Fray RG. Yeast m⁶A methylated mRNAs are enriched on translating ribosomes during meiosis, and under rapamycin treatment. *PLoS One.* 2015;10(7):e0132090.
- Dominissini D, Moshitch-Moshkovitz S, Schwartz S, Salmon-Divon M, Ungar L, Osenberg S, et al. Topology of the human and mouse m⁶A RNA methylomes revealed by m⁶A-seq. *Nature.* 2012;7397:201–6.
- Zhong X, Hongying L, Bodi Z, Button JD, Vespa L, Herzog M, et al. MTA is an *Arabidopsis* messenger RNA adenosine methylase and interacts with a homolog of a sex-specific splicing factor. *Plant Cell.* 2008;20:1278–88.
- Meyer KD, Saletore Y, Zumbo P, Elemento O, Mason CE, Jaffrey SR. Comprehensive analysis of mRNA methylation reveals enrichment in 3' UTRs and near stop codons. *Cell.* 2012;7:1635–46.
- Keene JD, Komisarow JM, Friedersdorf MB. RIP-Chip: the isolation and identification of mRNAs, microRNAs and protein components of ribonucleoprotein complexes from cell extracts. *Nat Protoc.* 2006;1:302–7.
- Dominissini D, Moshitch-Moshkovitz S, Salmon-Divon M, Amariglio N, Rechavi G. Transcriptome-wide mapping of N⁶-methyladenosine by m⁶A-seq based on immunocapturing and massively parallel sequencing. *Nat Protoc.* 2013;1:176–89.

11. Fustin JM, Doi M, Yamaguchi Y, Hida H, Nishimura S, Yoshida M, et al. RNA-methylation-dependent RNA processing controls the speed of the circadian clock. *Cell*. 2013;155:793–806.
12. Li YL, Wang XL, Li CP, Hu SN, Yu J, Song SH. Transcriptome-wide N6-methyladenosine profiling of rice callus and leaf reveals the presence of tissue-specific competitors involved in selective mRNA modification. *RNA Biol*. 2014;11(9):1180–8.
13. Luo GZ, MacQueen A, Zheng G, Duan H, Dore LC, Lu Z, et al. Unique features of the m6A methylome in *Arabidopsis thaliana*. *Nat Commun*. 2014; 5:5630.
14. Csepány T, Lin A, Baldick Jr CJ, Beemon K. Sequence specificity of mRNA N6-adenosine methyltransferase. *J Biol Chem*. 1990;265:20117–22.
15. Schledzewski K, Brinkmann H, Mendel RR. Phylogenetic analysis of components of the eukaryotic vesicle transport system reveals a common origin of adaptor protein complexes 1, 2, and 3 and the F subcomplex of the coatamer COPI. *J Mol Evol*. 1999;6:770–8.
16. Footitt S, Slocombe SP, Larner V, Kurup S, Wu Y, Larson T, et al. Control of germination and lipid mobilization by COMATOSE, the *Arabidopsis* homologue of human ALDP. *EMBO J*. 2002;12:2912–22.
17. Bedhomme M, Hoffmann M, McCarthy EA, Gambonnet B, Moran RG, Rébeillé F, et al. Folate metabolism in plants: an *Arabidopsis* homolog of the mammalian mitochondrial folate transporter mediates folate import into chloroplasts. *J Biol Chem*. 2005;41:34823–31.
18. Heyndrickx KS, Vandepoel K. Systematic identification of functional plant modules through the integration of complementary data sources. *Plant Physiol*. 2012;159:884–901.
19. Jammes F, Song C, Shin D, Munemasa S, Takeda K, Gu D, et al. MAP kinases MPK9 and MPK12 are preferentially expressed in guard cells and positively regulate ROS-mediated ABA signaling. *Proc Natl Acad Sci U S A*. 2009;48:20520–5.
20. Aranda-Sicilia MN, Cagnac O, Chanroj S, Sze H, Rodríguez-Rosales MP, Venema K. *Arabidopsis* KEA2, a homolog of bacterial KefC, encodes a K(+)/H(+) antiporter with a chloroplast transit peptide. *Biochim Biophys Acta*. 2012;9:2362–71.
21. Tsuchi R, Ditengou FA, Sumi Y, Teale W, Palme K, Okada K. NO VEIN mediates auxin-dependent specification and patterning in the *Arabidopsis* embryo, shoot, and root. *Plant Cell*. 2009;10:3133–51.
22. Charrier B, Champion A, Henry Y, Kreis M. Expression profiling of the whole *Arabidopsis* shaggy-like kinase multigene family by real-time reverse transcriptase-polymerase chain reaction. *Plant Physiol*. 2002;2:577–90.
23. Lellis AD, Kasschau KD, Whitham SA, Carrington JC. Loss-of-susceptibility mutants of *Arabidopsis thaliana* reveal an essential role for eIF(iso)4E during potyvirus infection. *Curr Biol*. 2002;12:1046–51.
24. Kawamura Y, Uemura M. Mass spectrometric approach for identifying putative plasma membrane proteins of *Arabidopsis* leaves associated with cold acclimation. *Plant J*. 2003;2:141–54.
25. Sarry JE, Kuhn L, Ducruix C, Lafaye A, Junot C, Hugouvieux V, et al. The early responses of *Arabidopsis thaliana* cells to cadmium exposure explored by protein and metabolite profiling analyses. *Proteomics*. 2006;7:2180–98.
26. Teotia S, Lamb RS. The paralogous genes *RADICAL-INDUCED CELL DEATH1* and *SIMILAR TO RCD ONE1* have partially redundant functions during *Arabidopsis* development. *Plant J*. 2008;1:29–41.
27. Chen LT, Luo M, Wang YY, Wu K. Involvement of *Arabidopsis* histone deacetylase HDA6 in ABA and salt stress response. *J Exp Bot*. 2010;12:3345–53.
28. Kindgren P, Kremnev D, Blanco NE, de Dios Barajas López J, Fernández AP, Tellgren-Roth C, et al. The plastid redox insensitive 2 mutant of *Arabidopsis* is impaired in PEP activity and high light-dependent plastid redox signalling to the nucleus. *Plant J*. 2012;2:279–91.
29. Yang S, Zeng X, Li T, Liu M, Zhang S, Gao S, et al. AtACD1, an ABC1-like kinase gene, is involved in chlorophyll degradation and the response to photooxidative stress in *Arabidopsis*. *J Exp Bot*. 2012;63(10):3959–73.
30. Zhang X, Wang C, Zhang Y, Sun Y, Mou Z. The *Arabidopsis* mediator complex subunit positively regulates salicylate-mediated systemic acquired resistance and jasmonate/ethylene-induced defense pathways. *Plant Cell*. 2012;10:4294–309.
31. Pu L, Liu MS, Kim SY, Chen LF, Fletcher JC, Sung ZR. EMBRYONIC FLOWER1 and ULTRAPETALA1 act antagonistically on *Arabidopsis* development and stress response. *Plant Physiol*. 2013;2:812–30.
32. Shrestha B, Guragain B, Sridhar VV. Involvement of co-repressor LUH and the adapter proteins SLK1 and SLK2 in the regulation of abiotic stress response genes in *Arabidopsis*. *BMC Plant Biol*. 2014;14:54.
33. Lee SJ, Lee MH, Kim JI, Kim SY. *Arabidopsis* putative MAP kinase kinase kinases Raf10 and Raf11 are positive regulators of seed dormancy and ABA response. *Plant Cell Physiol*. 2015;1:84–97.
34. Zolman BK, Silva ID, Bartel B. The *Arabidopsis* pxa1 mutant is defective in an ATP-binding cassette transporter-like protein required for peroxisomal fatty acid beta-oxidation. *Plant Physiol*. 2001;3:1266–78.
35. Nito K, Kamigaki A, Kondo M, Hayashi M, Nishimura M. Functional classification of *Arabidopsis* peroxisome biogenesis factors proposed from analyses of knockdown mutants. *Plant Cell Physiol*. 2007;6:763–74.
36. Attallah CV, Welchen E, Martin AP, Spinelli SV, Bonnard G, Palatnik JF, et al. Plants contain two SCO proteins that are differentially involved in cytochrome c oxidase function and copper and redox homeostasis. *J Exp Bot*. 2011;12:4281–94.
37. Hare PD, Moller SG, Huang LF, Chua NH. LAF3, a novel factor required for normal phytochrome A signaling. *Plant Physiol*. 2003;4:1592–604.
38. Parker G, Schofield R, Sundberg B, Turner S. Isolation of COV1, a gene involved in the regulation of vascular patterning in the stem of *Arabidopsis*. *Development*. 2003;10:2139–48.
39. van Leeuwen W, Okrész L, Bögre L, Munnik T. Learning the lipid language of plant signalling. *Trends Plant Sci*. 2004;8:378–84.
40. Caryl AP, Armstrong SJ, Jones GH, Franklin FC. A homologue of the yeast HOP1 gene is inactivated in the *Arabidopsis* meiotic mutant *asy1*. *Chromosoma*. 2000;109(1–2):62–71.
41. Kanno T, Bucher E, Daxinger L, Huettel B, Böhmendorfer G, Gregor W, et al. A structural-maintenance-of-chromosomes hinge domain-containing protein is required for RNA-directed DNA methylation. *Nat Genet*. 2008;40(5):670–5.
42. Campi M, D'Andrea L, Emiliani J, Casati P. Participation of chromatin-remodeling proteins in the repair of ultraviolet-B-damaged DNA. *Plant Physiol*. 2012;158(2):981–95.
43. Liu Y, Deng Y, Li G, Zhao J. Replication factor C1 (RFC1) is required for double-strand break repair during meiotic homologous recombination in *Arabidopsis*. *Plant J*. 2013;73:154–65.
44. Hanada K, Zhang X, Borevitz JO, Li WH, Shiu SH. A large number of novel coding small open reading frames in the intergenic regions of the *Arabidopsis thaliana* genome are transcribed and/or under purifying selection. *Genome Res*. 2007;5:632–40.
45. Habu Y, Mathieu O, Tariq M, Probst AV, Smathajitt C, Zhu T, et al. Epigenetic regulation of transcription in intermediate heterochromatin. *EMBO Rep*. 2006;12:1279–84.
46. Yaish MW, Peng M, Rothstein SJ. AtMBD9 modulates *Arabidopsis* development through the dual epigenetic pathways of DNA methylation and histone acetylation. *Plant J*. 2009;1:123–35.
47. Joukov V, Groen AC, Prokhorova T, Gerson R, White E, Rodriguez A, et al. The BRCA1/BARD1 heterodimer modulates ran-dependent mitotic spindle assembly. *Cell*. 2006;3:539–52.
48. Liu Y, Wang F, Zhang H, He H, Ma L, Deng XW. Functional characterization of the *Arabidopsis* ubiquitin-specific protease gene family reveals specific role and redundancy of individual members in development. *Plant J*. 2008;5:844–56.
49. Silady RA, Ehrhardt DW, Jackson K, Faulkner C, Oparka K, Somerville CR. The GRV2/RME-8 protein of *Arabidopsis* functions in the late endocytic pathway and is required for vacuolar membrane flow. *Plant J*. 2008;1:29–41.
50. Li G, Siddiqui H, Teng Y, Lin R, Wan XY, Li J, et al. Coordinated transcriptional regulation underlying the circadian clock in *Arabidopsis*. *Nat Cell Biol*. 2011;5:616–22.
51. Lei L, Li S, Du J, Bashline L, Gu Y. Cellulose synthase INTERACTIVE3 regulates cellulose biosynthesis in both a microtubule-dependent and microtubule-independent manner in *Arabidopsis*. *Plant Cell*. 2013;12:4912–23.
52. Fujimori K, Ohta D. Isolation and characterization of a histidine biosynthetic gene in *Arabidopsis* encoding a polypeptide with two separate domains for phosphoribosyl-ATP pyrophosphohydrolase and phosphoribosyl-AMP cyclohydrolase. *Plant Physiol*. 1998;1:275–83.
53. Han SK, Song JD, Noh YS, Noh B. Role of plant CBP/p300-like genes in the regulation of flowering time. *Plant J*. 2007;1:103–14.
54. Li MW, AuYeung WK, Lam HM. The GCN2 homologue in *Arabidopsis thaliana* interacts with uncharged tRNA and uses *Arabidopsis* eIF2 α molecules as direct substrates. *Plant Biol (Stuttg)*. 2013;1:13–8.

55. Lu DP, Christopher DA. Endoplasmic reticulum stress activates the expression of a sub-group of protein disulfide isomerase genes and AtbZIP60 modulates the response in *Arabidopsis thaliana*. *Mol Genet Genomics*. 2008;3:199–210.
56. Brooks MA, Dziembowski A, Quevillon-Cheruel S. Structure of the yeast Pml1 splicing factor and its integration into the RES complex. *Nucleic Acids Res*. 2009;37:129–43.
57. Chung T, Wang D, Kim CS, Yadegari R, Larkins BA. Plant SMU-1 and SMU-2 homologues regulate pre-mRNA splicing and multiple aspects of development. *Plant Physiol*. 2009;3:1498–512.
58. Hamada T, Igarashi H, Taguchi R, Fujiwara M, Fukao Y, Shimmen T, et al. The putative RNA-processing protein, THO2, is a microtubule-associated protein in tobacco. *Plant Cell Physiol*. 2009;4:801–11.
59. Kang CH, Feng Y, Vikram M, Jeong IS, Lee JR, Bahk JD, et al. *Arabidopsis thaliana* PRP40s are RNA polymerase II C-terminal domain-associating proteins. *Arch Biochem Biophys*. 2009;1:30–8.
60. Heazlewood JL, Tonti-Filippini JS, Gout AM, Day DA, Whelan J, Millar AH. Experimental analysis of the *Arabidopsis* mitochondrial proteome highlights signaling and regulatory components, provides assessment of targeting prediction programs, and indicates plant-specific mitochondrial proteins. *Plant Cell*. 2004;1:241–56.
61. Lee CP, Eubel H, O'Toole N, Millar AH. Heterogeneity of the mitochondrial proteome for photosynthetic and non-photosynthetic *Arabidopsis* metabolism. *Mol Cell Proteomics*. 2008;7:1297–316.
62. Zybailov B, Rutschow H, Friso GL, Rudella A, Emanuelsson O, Sun Q, et al. Sorting Signals, N-Terminal Modifications and Abundance of the Chloroplast Proteome. *PLoS One*. 2008;3(4), e1994.
63. Nikolovski N, Rubtsov D, Segura MP, Miles GP, Stevens TJ, Dunkley TP, et al. Putative glycosyltransferases and other plant Golgi apparatus proteins are revealed by LOPIT proteomics. *Plant Physiol*. 2012;2:1037–51.
64. Rosgaard L, Zygadlo A, Scheller HV, Mant A, Jensen PE. Insertion of the plant photosystem I subunit G into the thylakoid membrane. *FEBS J*. 2005;15:4002–10.
65. de Bianchi S, Dall'Osto L, Tognon G, Morosinotto T, Bassi R. Minor antenna proteins CP24 and CP26 affect the interactions between photosystem II subunits and the electron transport rate in grana membranes of *Arabidopsis*. *Plant Cell*. 2008;20(4):1012–28.
66. Sawchuk MG, Donner TJ, Head P, Scarpella E. Unique and overlapping expression patterns among members of photosynthesis-associated nuclear gene families in *Arabidopsis*. *Plant Physiol*. 2008;4:1908–24.
67. Woo HR, Kim JH, Nam HG, Lim PO. The delayed leaf senescence mutants of *Arabidopsis*, ore1, ore3, and ore9 are tolerant to oxidative stress. *Plant Cell Physiol*. 2004;7:923–32.
68. Mikkelsen MD, Thomashow MF. A role for circadian evening elements in cold-regulated gene expression in *Arabidopsis*. *Plant J*. 2009;2:328–39.
69. Zygadlo A, Jensen PE, Leister D, Scheller HV. Photosystem I lacking the PSI-G subunit has a higher affinity for plastocyanin and is sensitive to photodamage. *Biochim Biophys Acta*. 2005;2:154–63.
70. Ferro M, Brugièrè S, Salvi D, Seigneurin-Berny D, Court M, Moyet L, et al. AT_CHLORO, a comprehensive chloroplast proteome database with subplastidial localization and curated information on envelope proteins. *Mol Cell Proteomics*. 2010;6:1063–84.
71. Kwak JM, Mori IC, Pei ZM, Leonhardt N, Torres MA, Dangl JL, et al. NADPH oxidase AtrbohD and AtrbohF genes function in ROS-dependent ABA signaling in *Arabidopsis*. *EMBO J*. 2003;11:2623–33.
72. Gillissen B, Bürkle L, André B, Kühn C, Rentsch D, Brandl B, et al. A new family of high-affinity transporters for adenine, cytosine, and purine derivatives in *Arabidopsis*. *Plant Cell*. 2000;2:291–300.
73. Diener AC, Gaxiola RA, Fink GR. *Arabidopsis* ALF5, a multidrug efflux transporter gene family member, confers resistance to toxins. *Plant Cell*. 2001;7:1625–38.
74. Mäser P, Thomine S, Schroeder JI, Ward JM, Hirschi K, Sze H, et al. Phylogenetic relationships within cation transporter families of *Arabidopsis*. *Plant Physiol*. 2001;4:1646–67.
75. Pertry I, Václavíková K, Depuydt S, Galuszka P, Spíchal L, Temmerman W, et al. Identification of *Rhodococcus fascians* cytokinins and their modus operandi to reshape the plant. *Proc Natl Acad Sci U S A*. 2009;3:929–34.
76. Bae MS, Cho EJ, Choi EY, Park OK. Analysis of the *Arabidopsis* nuclear proteome and its response to cold stress. *Plant J*. 2003;5:652–63.
77. Sels J, Mathys J, De Coninck BM, Cammue BP, De Bolle MF. Plant pathogenesis-related (PR) proteins: a focus on PR peptides. *Plant Physiol Biochem*. 2008;11:941–50.
78. Wormit A, Butt SM, Chairam I, McKenna JF, Nunes-Nesi A, Kjaer L, et al. Osmosensitive changes of carbohydrate metabolism in response to cellulose biosynthesis inhibition. *Plant Physiol*. 2012;1:105–17.
79. Yang Y, Xu R, Ma CJ, Vlot AC, Klessig DF, Pichersky E. Inactive methyl indole-3-acetic acid ester can be hydrolyzed and activated by several esterases belonging to the AtMES esterase family of *Arabidopsis*. *Plant Physiol*. 2008;3:1034–45.
80. Tanaka H, Ishikawa M, Kitamura S, Takahashi Y, Soyano T, Machida C, et al. The AtNACK1/HINKEL and STUD/TETRASPORE/AtNACK2 genes, which encode functionally redundant kinesins, are essential for cytokinesis in *Arabidopsis*. *Genes Cells*. 2004;12:1199–211.
81. Schmid M, Davison TS, Henz SR, Pape UJ, Demar M, Vingron M, et al. A gene expression map of *Arabidopsis thaliana* development. *Nat Genet*. 2005;5:501–6.
82. Borg M, Brownfield L, Khatib H, Sidorova A, Lingaya M, Twell D. The R2R3 MYB transcription factor DUO1 activates a male germline-specific regulon essential for sperm cell differentiation in *Arabidopsis*. *Plant Cell*. 2011;2:534–49.
83. Reňák D, Dupl'áková N, Honys D. Wide-scale screening of T-DNA lines for transcription factor genes affecting male gametophyte development in *Arabidopsis*. *Sex Plant Reprod*. 2012;1:39–60.
84. Lee JH, Yoon HJ, Terzaghi W, Martinez C, Dai M, Li J, et al. DWA1 and DWA2, two *Arabidopsis* DWD protein components of CUL4-based E3 ligases, act together as negative regulators in ABA signal transduction. *Plant Cell*. 2010;6:1716–32.
85. Froehlich JE, Wilkerson CG, Ray WK, McAndrew RS, Osteryoung KW, Gage DA, et al. Proteomic study of the *Arabidopsis thaliana* chloroplast envelope membrane utilizing alternatives to traditional two-dimensional electrophoresis. *J Proteome Res*. 2003;4:413–25.
86. Carroll AJ, Heazlewood JL, Ito J, Millar AH. Analysis of the *Arabidopsis* cytosolic ribosome proteome provides detailed insights into its components and their post-translational modification. *Mol Cell Proteomics*. 2008;2:347–69.
87. Mähönen AP, Higuchi M, Törmäkangas K, Miyawaki K, Pischke MS, Sussman MR, et al. Cytokinins regulate a bidirectional phosphorelay network in *Arabidopsis*. *Curr Biol*. 2006;11:1116–22.
88. Suzuki T, Miwa K, Ishikawa K, Yamada H, Aiba H, Mizuno T. The *Arabidopsis* sensor His-kinase, AHK4, can respond to cytokinins. *Plant Cell Physiol*. 2001;2:107–13.
89. Gruis DF, Selinger DA, Curran JM, Jung R. Redundant proteolytic mechanisms process seed storage proteins in the absence of seed-type members of the vacuolar processing enzyme family of cysteine proteases. *Plant Cell*. 2002;11:2863–82.
90. Yang H, Matsubayashi Y, Nakamura K, Sakagami Y. Diversity of *Arabidopsis* genes encoding precursors for phyto-sulfokine, a peptide growth factor. *Plant Physiol*. 2001;3:842–51.
91. Etchells JP, Provost CM, Turner SR. Plant vascular cell division is maintained by an interaction between PXY and ethylene signalling. *PLoS Genet*. 2012;11, e1002997.
92. Gidda SK, Miersch O, Levitin A, Schmidt J, Wasternack C, Varin L. Biochemical and molecular characterization of a hydroxyjasmonate sulfotransferase from *Arabidopsis thaliana*. *J Biol Chem*. 2003;20:17895–900.
93. Libault M, Wan J, Czechowski T, Udvardi M, Stacey G. Identification of 118 *Arabidopsis* transcription factor and 30 ubiquitin-ligase genes responding to chitin, a plant-defense elicitor. *Mol Plant Microbe Interact*. 2007;8:900–11.
94. Huibers RP, de Jong M, Dekter RW, Van den Ackerveken G. Disease-specific expression of host genes during downy mildew infection of *Arabidopsis*. *Mol Plant Microbe Interact*. 2009;9:1104–15.
95. Ahlfors R, Brosché M, Kollist H, Kangasjärvi J. Nitric oxide modulates ozone-induced cell death, hormone biosynthesis and gene expression in *Arabidopsis thaliana*. *Plant J*. 2009;1:1–12.
96. Liu J, Elmore JM, Lin ZJ, Coaker G. A receptor-like cytoplasmic kinase phosphorylates the host target RIN4, leading to the activation of a plant innate immune receptor. *Cell Host Microbe*. 2011;2:137–46.
97. Ogawa T, Ueda Y, Yoshimura K, Shigeoka S. Comprehensive analysis of cytosolic Nudix hydrolases in *Arabidopsis thaliana*. *J Biol Chem*. 2005;26:25277–83.
98. Brown DM, Zhang Z, Stephens E, Dupree P, Turner SR. Characterization of IRX10 and IRX10-like reveals an essential role in glucuronoxylan biosynthesis in *Arabidopsis*. *Plant J*. 2009;4:732–46.

99. Thines B, Katsir L, Melotto M, Niu Y, Mandaokar A, Liu G, et al. JAZ repressor proteins are targets of the SCF(COI1) complex during jasmonate signalling. *Nature*. 2007;7154:661–5.
100. Ghelis T, Bolbach G, Clodic G, Habricot Y, Miginiac E, Sotta B, et al. Protein tyrosine kinases and protein tyrosine phosphatases are involved in abscisic acid-dependent processes in *Arabidopsis* seeds and suspension cells. *Plant Physiol*. 2008;3:1668–80.
101. Salzman RA, Fujita T, Zhu-Salzman K, Hasegawa PM, Bressan RA. An improved RNA isolation method for plant tissues containing high levels of phenolic compounds or carbohydrates. *Plant Mol Biol Rep*. 1999;17:11–7.
102. Azevedo H, Lino-Neto T, Tavares RM. An improved method for high quality RNA isolation from needles of adult maritime pine trees. *Plant Mol Biol Rep*. 2003;21:333–8.
103. Bodi Z, Zhong S, Mehra S, Song J, Graham N, Li H, et al. Adenosine methylation in *Arabidopsis* mRNA is associated with the 3' End and reduced levels cause developmental defects. *Front Plant Sci*. 2012;3:48. eCollection 2012.
104. Alberts B, Johnson A, Lewis J, Raff M, Roberts K, Walter P. *Molecular biology of the cell*. 4th ed. New York, NY: Garland Science; 2002.
105. Dahlberg JE, Lund E. Does protein synthesis occur in the nucleus? *Curr Opin Cell Biol*. 2004;16:335–8.
106. Go YM, Jones DP. Redox compartmentalization in eukaryotic cells. *Biochim Biophys Acta*. 2008;1780(11):1273–90.
107. Lodish H, Berk A, Zipursky SL, Matsudaira P, Baltimore D, Darnell J. *Molecular Cell Biology*. 4th ed. New York, NY: W. H. Freeman; 2000.
108. Ochs RS. *Biochemistry*. Burlington, MA: Jones & Bartlett Learning; 2012.
109. Walter P, Blobel G. Translocation of proteins across the endoplasmic reticulum. II. Signal recognition protein (SRP) mediates the selective binding to microsomal membranes of in-vitro-assembled polysomes synthesizing secretory protein. *J Cell Biol*. 1981;91:551–6.
110. Walter P, Blobel G. Translocation of proteins across the endoplasmic reticulum III. Signal recognition protein (SRP) causes signal sequence-dependent and site-specific arrest of chain elongation that is released by microsomal membranes. *J Cell Biol*. 1981;91:557–61.
111. Stephens SB, Nicchitta CV. Divergent regulation of protein synthesis in the cytosol and endoplasmic reticulum compartments of mammalian cells. *Mol Biol Cell*. 2008;2:623–32.
112. Niu Y, Zhao X, Wu YS, Li MM, Wang XJ, Yang YG. N^6 -methyl-adenosine (m^6A) in RNA: an old modification with a novel epigenetic function. *Genomics Proteomics Bioinformatics*. 2013;1:8–17.
113. Mohammad HP, Baylin SB. Linking cell signaling and the epigenetic machinery. *Nat Biotechnol*. 2010;10:1033–8.
114. Perry RP, Kelley DE, Friderici K, Rottman F. The methylated constituents of L cell messenger RNA: evidence for an unusual cluster at the 5' terminus. *Cell*. 1975;4:387–94.
115. Meyer KD, Jaffrey SR. The dynamic epitranscriptome: N^6 -methyladenosine and gene expression control. *Nat Rev Mol Cell Biol*. 2014;5:313–26.
116. Fu Y, Dominissini D, Rechavi G, He C. Gene expression regulation mediated through reversible m^6A RNA methylation. *Nat Rev Genet*. 2014;5:293–306.
117. Stoltzfus CM, Dane RW. Accumulation of spliced avian retrovirus mRNA is inhibited in S-adenosylmethionine-depleted chicken embryo fibroblasts. *J Virol*. 1982;42:918–31.
118. Camper SA, Albers RJ, Coward JK, Rottman FM. Effect of undermethylation on mRNA cytoplasmic appearance and half-life. *Mol Cell Biol*. 1984;4:538–43.
119. Tuck MT, Wiehl PE, Pan T. Inhibition of 6-methyladenine formation decreases the translation efficiency of dihydrofolate reductase transcripts. *Int J Biochem Cell Biol*. 1999;31:837–51.
120. DeLeon SBT, Davidson EH. Gene regulation: Gene control network in development. *Annu Rev Biophys Biomol Struct*. 2007;36:191–212.
121. Rapaport F, Khanin R, Liang Y, Pirun M, Krek A, Zumbo P, et al. Comprehensive evaluation of differential gene expression analysis methods for RNA-seq data. *Genome Biol*. 2013;9:R95.
122. Wang Y, Zhang WZ, Song LF, Zou JJ, Su Z, Wu WH. Transcriptome analyses show changes in gene expression to accompany pollen germination and tube growth in *Arabidopsis*. *Plant Physiol*. 2008;3:1201–11.
123. McMahon MJ, Kofranek AM, Rubatzky VE. *Plant Science*. Upper Saddle River, NJ: Pearson Education, Inc.; 2011.
124. Bengough AG, Bransby MF, Hans J, McKenna SJ, Roberts TJ, Valentine TA. Root responses to soil physical conditions; growth dynamics from field to cell. *J Exp Bot*. 2006;2:437–47.
125. Feschotte C. Transposable elements and the evolution of regulatory networks. *Nat Rev Genet*. 2008;9:397–405.
126. Schnable PS, Ware D, Fulton RS, Stein JC, Wei F, Pasternak S, et al. The B73 maize genome: complexity, diversity, and dynamics. *Science*. 2009;5956:1112–5.
127. Bucher E, Reinders J, Mirouze M. Epigenetic control of transposon transcription and mobility in *Arabidopsis*. *Curr Opin Plant Biol*. 2012;5:503–10.
128. Belancio VP, Hedges DJ, Deininger P. Mammalian non-LTR retrotransposons: for better or worse, in sickness and in health. *Genome Res*. 2008;18:343–58.
129. Slotkin RK, Martienssen R. Transposable elements and the epigenetic regulation of the genome. *Nat Rev Genet*. 2007;8:272–85.
130. van de Lagemaat LN, Landry JR, Mager DL, Medstrand P. Transposable elements in mammals promote regulatory variation and diversification of genes with specialized functions. *Trends Genet*. 2003;19:530–6.
131. Marino-Ramirez L, Lewis KC, Landsman D, Jordan IK. Transposable elements donate lineagespecific regulatory sequences to host genomes. *Cytogenet Genome Res*. 2005;110:333–41.
132. Kang SG, Liu WH, Lu P, Jin HY, Lim HW, Shepherd J, et al. MicroRNAs of the miR-17 ~92 family are critical regulators of T(FH) differentiation. *Nat Immunol*. 2013;8:849–57.
133. Gambino G, Perrone I, Gribaudo I. A rapid and effective method for RNA extraction from different tissues of grapevine and other woody plants. *Phytochem Anal*. 2008;19:520–5.
134. Kim D, Pertea G, Trapnell C, Pimentel H, Kelley R, Salzberg SL. TopHat2: accurate alignment of transcriptomes in the presence of insertions, deletions and gene fusions. *Genome Biol*. 2013;4:R36.
135. Li H, Handsaker B, Wysoker A, Fennell T, Ruan J, Homer N, et al. The sequence alignment/map format and SAMtools. *Bioinformatics*. 2009;16:2078–9.
136. Liao Y, Smyth GK, Shi W. featureCounts: an efficient general purpose program for assigning sequence reads to genomic features. *Bioinformatics*. 2014;7:923–30.
137. Robinson JT, Thorvaldsdóttir H, Winckler W, Guttman M, Lander ES, Getz G, et al. Integrative Genomics Viewer. *Nat Biotechnol*. 2011;1:24–6.
138. Trapnell C, Williams BA, Pertea G, Mortazavi A, Kwan G, van Baren MJ, et al. Transcript assembly and quantification by RNA-Seq reveals unannotated transcripts and isoform switching during cell differentiation. *Nat Biotechnol*. 2010;5:511–5.
139. Berardini TZ, Mundodi S, Reiser R, Huala E, Garcia-Hernandez M, Zhang P, et al. Functional annotation of the *Arabidopsis* genome using controlled vocabularies. *Plant Physiol*. 2004;2:1–11.

Submit your next manuscript to BioMed Central and we will help you at every step:

- We accept pre-submission inquiries
- Our selector tool helps you to find the most relevant journal
- We provide round the clock customer support
- Convenient online submission
- Thorough peer review
- Inclusion in PubMed and all major indexing services
- Maximum visibility for your research

Submit your manuscript at
www.biomedcentral.com/submit

